Ministry of Higher Education & Scientific Research
Ninevah University
College of Electronics Engineering
Communication Engineering Department

Investigation and Simulation of Non-Orthogonal Multiple Access over mmWave Channels

By

Ahmad Attallah Saleh

M.Sc. Thesis

In

Communication Engineering

Supervised by

Dr. Mohamad Abdulrahman Alhabbar

2023 A.D.   **1445 A.H.**

Investigation and Simulation of Non-Orthogonal Multiple Access over mmWave Channels

A Thesis Submitted

By

Ahmad Attallah Saleh

To

The Council of the College of Electronic Engineering

Ninevah University

As a Partial Fulfillment of the Requirements

for the Degree of Master of Science

In

Communication Engineering

Supervised by

Dr. Mohamad Abdulrahman Alhabbar

2023 A.D.   **1445 A.H.**

بِسْمِ اللَّهِ الرَّحْمَٰنِ الرَّحِيمِ

(قُلْ هَلْ يَسْتَوِي الَّذِينَ يَعْلَمُونَ وَالَّذِينَ لَا يَعْلَمُونَ إِنَّمَا يَتَذَكَّرُ أُولُوا الْأَلْبَابِ)

صَدَقَ اللهُ العَظِيمُ

سورة الزمر ـ ايه (9)

Committee Certification

We the examining committee, certify that we have read this thesis entitled **"*Investigation and Simulation of Non-Orthogonal Multiple Access over mmWave Channels*"** and have examined the postgraduate student (**Ahmed Attallah Saleh**) in its contents and that in our opinion; it meets the standards of a thesis for the degree of Master of Science in Communication Engineering.

Signature:

Name: Dr. Dia Mohamad Ali

Head of the committee

Date: /   / 2023

Signature:

Name: **Dr. Saad Ahmed Ayoob**

Member

Date: /   / 2023

Signature:

Name: Dr. Safwan Hafeedh Younus

Member

Date: /   / 2023

Signature:

Name: **Dr. Mohamad A. Alhabbar**

Member and Supervisor

Date: /   / 2023

The college council, in it's ………… meeting on   /   / 2023, has decided to award the degree of Master of Science in Communication Engineering to the candidate.

Signature:

Name:Prof. Dr. Khaled Khalil Muhammad

Dean of the College

Date: /   / 2023

Signature:

Name: Dr. Bilal A. Jebur

Council registrar

Date: /   / 2023

DEDICATION

I dedicate this work to my family, especially to my mother because she always prays for me to be successful in life, as well as to my wife, my brothers, my friends, and especially to those who support me until completed this work.

Acknowledgments

Abstract

In this thesis, non-orthogonal multiple access (NOMA) with multiple-input multiple-output (MIMO) over millimeter wave (mmWave) channels is investigated and characterized. These two techniques are merged to serve multi-users in the next generation of wireless communication. The NOMA multiplexing technique has witnessed lots of interest due to its ability to enhance spectral efficiency significantly. Moreover, massive MIMO is the mechanism of transmission over tens and hundreds number of antennas, which also improves the system throughputs and reduced the required transmitted power. Furthermore, the use of mmWave as a promising uncongested band would enhance the system performance, increase the transmission bandwidth and reduce the latency.

Two aspects are proposed and investigated in this thesis, the first aspect is the employing of cooperative relays, in the decode-and-forward (DF) mode, to tackle the path-loss issue inherent in the mmWave bands, while the second one is to use beamforming with massive MIMO to increase the signal of interest and reduce the interference at each user terminal.

In the first aspect, two links with different frequency bands are considered to serve users by a base station (BS) via DF cooperative relays. Backhaul and access links are proposed with sub-6 GHz and mmWave bands, respectively. The NOMA is employed in the backhaul link to transmit a superposed signal in the power domain simultaneously using the same band. The superposed signals, which contain two signals that differ in power allocation factors (PAFs), are constructed for two selected DF relays in the BS. The two relays are chosen among several relays to be serviced by the BS via utilizing a pairing algorithm depending on different users' circumstances. The furthest DF relay detects the incoming NOMA signal directly, while the nearest one applies successive interference cancellation (SIC) before

extracting its signal. Each DF relay forwards the detected signals toward their intended users over mmWave channels. Furthermore, three performance metrics are utilized to evaluate the system's performance, which are the outage probability, the spectral efficiency, and the bit-error rate. Moreover, the comparisons between two mmWave bands in the access link, which are 28GHz and 73GHz, are obtained to demonstrate the superiority of 28 GHz in the three-performance metrics.

In the second aspect, massive MIMO with NOMA is considered to serve multiple users wirelessly over mmWave channels, in which a BS with tens of antennas is proposed to provide services to users in the coverage area by applying zero-forcing (ZF) and maximum ratio transmission (MRT) beamforming techniques. The BS first divides the area into clusters which contain only two users via applying a pairing algorithm, then NOMA is applied to the two users by providing different power allocation factors for satisfying user fairness, and depending on users' circumstances. The achievable throughput for each user in the cluster along with the sum-rate provided by the BS are analyzed and evaluated for the two beamforming mechanisms. The results are obtained for different numbers of BS antennas over different combinations of power allocation coefficients. The simulation results reveal the improvement obtained by increasing the antennas in the BS. Additionally, the two beamforming methods introduce similar throughput when the same parameters are considered, with slight outperforming of MRT in the outage portability.

TABLE OF CONTENTS

LIST OF FIGURES

LIST OF TABLES

LIST OF ABBREVIATIONS

Abbreviation	Name
3D	Three Dimensions
4G	Fourth Generation
5G	Fifth Generation
ABG	alpha-beta-gamma
ACS	Antenna Clustering Scheme
AF	Amplify and Forward
ANN	Artificial Neural Network
AWGN	Additive White Gaussian Noise
BER	Bit Error Rate
BS	Base Station
BW	Bandwidth
CapMC	Capacity-Maximization Criterion
CCR	Conventional Cooperative Relaying
CF	Compressed and Forwards
CI	Close-In
CovMC	Coverage-Maximization Criterion
CSI	Channel State Information
DAF	Decode Amplify and Forwards
DF	Decode and Forwards
E2E	End to End
FDMA	Frequency Division Multiple Access
FI	Floating Intercept
FSPL	Free Space Path Loss
GSVD	Generalized Singular Value Decomposition

HB	Hybrid Beamforming
HP	Hybrid Precoding
HPBW	Half Beamwidth
LOS	Line of Sight
LTE	Long Term Evolution
MIMO	Multiple Input and Multiple Output
MMSE	Minimum Mean Squared Error
mmWave	Millimeter-wave
MRT	Maximum Ratio Transmission
MS	Mobile Station
NLOS	Non-Line of Sight
NOMA	Non Orthogonal Multiple Access
OAM	Orbital Angular Momentum
OMA	Orthogonal Multiple Access
PA	Power Allocation
PAF	Power Allocation Factor
PL	Path Loss
PLC	Power Line Communication
PLE	Path Loss Exponent
PS	Power Splitting
QoS	Quality of Service
QPSK	Quadrature Phase Shift Keying
RF	Radio Frequency
Rx	Receiver
SC	Superposition Coding
SDMA	Space Division Multiple Access
SIC	Successive Interference Cancelation
SINR	Signal to Interference plus Noise Ratio

SNR	Signal-to-Noise Ratio
SWIDEH	Simultaneous Wireless Information Decoding and Energy Harvesting
SWIPT	Simultaneously Wireless Information and Power Transfer
TDMA	Time division multiple access
Tx	Transmitter
U	User
ZF	Zero Forcing

LIST OF SYMBOLS

Symbol	Name
H	Channel Coefficient matrix
β	Path loss Exponent for Floating Intercept model
P	Available Power at the Transmitter
B	System Bandwidth
C	channel capacity
R	System Throughput
α	Power Allocation Factor
σ^2	Variance of Noise
d	Distance from Base Station to the User
N	Noise
Ω	Signal-to-Noise Ratio
γ	Signal-to-Interference-Plus-Noise Ratio
f	Operating Frequency
W	Additive White Gaussian Noise
n	Path Loss Coefficient for Close-In model
SE	Spectral Efficiency
G	Gain
δ	Floating Intercept Coefficient

CHAPTER ONE

INTRODUCTION

1.1 Overview

Wireless communications have become more prevalent and have permeated every facet of modern life, resulting in constant advancement and qualitative leaps in the communications industry. The lack of spectrum, the need to communicate with a large number of users, and the need for high data speeds and reliability are some of the challenges. As with previous generations, the urgent need for more services led to the development of the fifth generation (5G) and beyond wireless networks. Non-orthogonal multiple access (NOMA) can fulfill these objectives [1]. By using the same band of frequency simultaneously for numerous users in the cell, NOMA can be extremely helpful in achieving massive connections. By using the power allocation approach, in transmissions between the base station (BS) and the mobile station (MS) in the downlink and uplink phases. User fairness, secure connectivity, and spectral efficiency can all be satisfied by NOMA.

To allow several users to share the same time-frequency resources, NOMA is built on the superposition coding principle. This allows users to do so by allocating different power levels or codes. Each user is given his own frequency or time slot in conventional orthogonal multiple access (OMA) schemes like frequency division multiple access (FDMA) or time division multiple access (TDMA).

Millimeter-wave (mmWave) bands have attracted a lot of interest as a potential supplementary spectrum band for 5G and beyond cellular networks because standard microwave bands are so limited in the spectrum[2]. The mmWave band is referred to as the area of the electromagnetic spectrum with

wavelengths between 10 mm and 1 mm and falling between 30 GHz and 300 GHz. The data rate and capacity of a mmWave communication system can be increased by handling multiple gigahertz of bandwidth [3].

The BS and MS systems needed new antenna architectural concepts for mmWave frequencies to successfully implement a fundamental element of 5G wireless networks, a beam-steerable phased array antenna, and to do it at a low cost. Sharp beamforming or multiple-input multiple-output (MIMO) technologies are also made possible by the short wavelength of mmWave, which makes it possible for mmWave antennas to be made smaller than those used for conventional cellular frequency waves [4]. When tens, hundreds, or even thousands of antennas are typically used in single antenna arrays then the systems are called massive MIMO. Massive MIMO is a technology that uses numerous antennas at the base station to provide service to many users at once. Massive MIMO can enhance the system's coverage, capacity, and overall performance by using spatial multiplexing and beamforming techniques. A wide antenna array improves the signal-to-noise ratio (SNR), reduces interference, and offers more reliable link performance.

There are many advantages when NOMA is used over mmWave channels. Firstly, by assigning various power levels to various users, the extensive bandwidth present in the mmWave spectrum may be effectively exploited. As a result, spectral efficiency and system capacity can be improved. Additionally, it is possible to successfully leverage the mmWave broadcasts' narrow beams to facilitate the simultaneous transmission and receipt of numerous user signals in the same time-frequency resources, significantly enhancing system performance.

To achieve high-quality communication links in mmWave-NOMA systems, beamforming techniques are essential. Beamforming makes it possible to create highly directional beams that may be precisely guided

toward the designated receivers, reducing user interference. NOMA can offer more degrees of freedom for multiple users to share the same resources by utilizing the spatial dimension through beamforming.

1.2 Literature Review

Many related works on the subject of NOMA and mmWave bands have been investigated in previous researches. In this section, the most relevant works to the proposed system in this thesis are reviewed, which include the following:

In 2003, M. Ghaddar et. al. presented wideband predicted results for indoor wireless communications operating at 37.2 GHz, based on verified ray-tracing modeling. The data analysis reveals that selecting the right location for the antenna in the indoor channel is crucial to minimize the interference caused by symbols [5].

In 2009, v. K. Sakarellos et. al. presented the physical models for the dual-hop system's outage performance statistics. The investigation included both transparent and regenerative radio relays that operate at frequencies over 10 GHz and meet the line-of-sight requirement. The performance of the outage has been thoroughly evaluated with geometrical and operational characteristics, various relay types, and various environmental circumstances [6].

In 2012, Salam Akoum et al. compared large mmWave cellular networks servicing one or more users per cell to conventional microwave systems to characterize the probability of coverage. Given that the two systems' coverage was comparable, mmWave frequencies' greater bandwidths can enable substantially faster data rates than microwave systems [7].

In 2013, Beomju Kim et al. suggested a NOMA-beamforming system to increase sum capacity. Because two users can share a single BF vector in the proposed NOMA- beamforming system, more users can be supported. Furthermore, by implementing the suggested clustering algorithm and efficient power allocation, which gives the ability to reduce inter-cluster and inter-user interferences, the proposed NOMA- beamforming's total capacity was increased in comparison to the traditional multiuser beamforming system while maintaining the weak user capacity [8].

Yuya Saito et al., in 2013 analyzed the system-level performance of NOMA while taking into account more useful cellular system features as well as some important long-term evolution (LTE) radio interface functionalities, such as frequency-domain scheduling, as well as NOMA-specific features like dynamic multi-user power allocation [9].

In 2014, Taehoon Kim et al. developed a mmWave-based small cell with multiple directional antennas and suggested an antenna clustering scheme (ACS) to enhance the small cell coverage. Additionally, they described two design criteria for a mmWave-based small cell: a capacity-maximization criterion (CapMC) and a coverage-maximization criterion (CovMC) [2].

In 2014, Jinho Choi discussed how to support a cell edge user in a NOMA channel by using two-point systems, which can provide an acceptable transmission rate to a cell edge user without decreasing the rates to users near to BSs [10].

In 2015, Kenichi Higuchi and Anass Benjebbour presented NOMA as a new and promising future radio access, using successive interference cancellation(SIC) at the receiver side to achieve better user fairness and system efficiency than OMA [11].

In 2015, Zhiguo Ding et al. studied a cooperative NOMA transmission technique that makes use of certain users in NOMA networks who have previous information. To illustrate the performance benefit of this cooperative NOMA method, analytical findings have been provided. In this study, fixed power allocation coefficients have been employed, and it is crucial to research the best power distribution for cooperative NOMA [12].

Linglong Dai et al., in 2015 discussed NOMA as a solution for 5G networks and beyond, NOMA is different from OMA. Through nonorthogonal resource allocation, NOMA can support a lot more users. Power-domain NOMA, multi-user shared access, sparse code multiple access, multiple access with low-density spreading, and pattern division multiple access are some of the dominant NOMA schemes that the current study divides into two categories: power-domain multiplexing and code-domain multiplexing [13].

In 2016, Shu Sun et al. discussed and compared two types of propagation path loss models, the close-in (CI) free space reference distance model and the alpha-beta-gamma(ABG) model for the design of 5G wireless communication systems [14].

Shimei Liu and Chao Zhang, in 2016 studied NOMA downlink multiuser beamforming system with limited channel state information (CSI) feedback. They incorporate the random beamforming and zero-forcing (ZF) beamforming into NOMA downlink multiuser and provide feedback in the form of channel direction information and a channel quality indicator that is provided over a limited rate channel by the potential users [15].

In 2016, Zhang Han et al. claimed that more than one user with identical resources might be chosen by using the user pairing algorithm approach. To ensure maximum capacity and user fairness, this algorithm chooses users based on various channel characteristics [16].

In 2017, Jinjin Men et al. studied the outage performance for downlink NOMA with imperfect CSI over Nakagami-m fading channels. The theoretical foundation for providing helpful advice in the real communication system design is the closed-form expressions for the exact and lower bound of the outage probability [17].

Khaled M. Rabie et al., in 2017 suggested NOMA for decode-and-forward (DF) cooperative relaying power line communication (PLC) systems to increase throughput and enhance user fairness. Additionally, they researched conventional cooperative relaying (CCR) PLC systems to objectively quantify the performance of the proposed system and compared the two systems' performance based on their average capacity [18].

In 2018, Zhen Luo et al. presented a robust hybrid beamforming scheme for mmWave amplify and forward (AF) MIMO relay networks. To establish an approximate average received SNR as the design criterion, the imperfect CSI with Gaussian-distributed errors is taken into consideration. The beamformers at various nodes can be optimized alternately using an iterative approach [19].

Mojtaba Ahmadi Almasi and Hani Mehrpouyan, in 2018 investigated the use of NOMA in hybrid beamforming (HB) multiuser systems to serve a high number of users. The HB-NOMA problem's sum-rate formulation is created first. The second step is the proposal of an efficient method to optimize the sum rate [20].

In 2018, K A I Yang et al. suggested a novel uniform beam selection technique or the mmWave massive MIMO-NOMA system. To discover the best channels for the users, they take advantage of the cross-correlation and channel sparsity of the users. The numerical outcomes have demonstrated how

the suggested technique may enhance not only spectrum and energy efficiency but also user computation [21].

Khagendra Belbase et al., in 2019 calculated the coverage probability of three NOMA relay selection cooperative mmWave schemes. Closest-to-source relay selection and closest-to-destination relay selection both exceed OMA. However, depending on transmit power level and relay density, coverage caused by a random relay could be worse than that of OMA. This study takes into account a place that is not connected to the source directly [22].

In 2019, Xiangbin Yu et al. investigated the energy efficiency optimization in a downlink multi-user mmWave-NOMA system with hybrid precoding (HP) by considering fully-connected and sub-connected HP architectures, and a suboptimal energy-efficient power allocation technique with low complexity is provided for the system. The user pairing method and two-step HP design are first given using the study of energy efficiency as a foundation. The digital ZF precoding is intended to remove inter-cluster interference for the strong users in all clusters, and the analog beamforming is specifically presented to increase performance. With the use of these findings, the energy efficiency maximization issue is then formalized, and the fractional programming theory may be used to split it into separate convex sub-problems [23].

In 2019, Lipeng Zhu et al. investigated the combination of NOMA and mmWave communications. The authors considered a downlink cellular, in which several users are served by BS with a single antenna using a single radio frequency (RF) chain and a sizable antenna array. To lower hardware costs and power usage, analog beamforming was used [24].

In 2020, Anthony Ngozichukwuka Uwaechia and Nor Muzlifah Mahyuddin discussed a thorough analysis of upcoming 5G mmWave propagation characteristics, including free-space path loss, rain and foliage-induced attenuation, material penetration loss, atmospheric-induced attenuation, and other propagation parameters. For the 5G channel modeling, radio frequency spectrum and legal challenges have been provided. The authors discussed mmWave communication, massive MIMO communication, multiple access, and performance analysis which represented the most challenging 5G systems communication scenarios [25].

In 2020, Ahmed Al Amin and Soo Young Shin proposed an orbital angular momentum-based MIMO (OAM-MIMO) to increase the channel capacity of downlink NOMA cellular communication. The user and sum capacities of the proposed NOMA-OAM-MIMO system are examined, and contrasted with those of other conventional schemes, such as OMA with OAM-MIMO multiplexing and traditional NOMA with MIMO [26].

In 2020, Yue Wang et al. studied the spectrum and energy efficiency of spectrum-shared NOMA-mmWave systems with massive MIMO, with emphasis on learning-aided real-time system optimization, optimal sensing resource allocation, high-performance, and low-complexity channel sensing, security and privacy providing [27].

In 2021, Joydev Ghosh et al. described and compared how NOMA and OMA work for mmWave massive MIMO-based wireless networks from the perspective of operating principles, the authors have shown that mmWave huge MIMO-NOMA can be implemented with adequate resource allocation and precoding, compared to MIMO-OMA, based communications can significantly enhance spectral efficiency, energy efficiency, and outage probability performances. Additionally, the OFDM-based MIMO-OMA systems' high peak-to-average power ratio issue can be resolved [28].

Meng Han et al. in 2021, studied the mmWave massive multi-user MIMO domain's mixed-structure DF relay systems. The goal of the hybrid beamforming design is to increase the sum rate between the users and the source node. An effective sorted serial design method is suggested to design the analog beamforming of each node to resolve this difficult hybrid beamforming design problem [29].

In 2022, Joonpyo Hong et al. suggested a simple user scheduling, power allocation, and beam activation mechanism to maximize network utility. To simplify the original problem and reduce its computational complexity, several heuristic but useful approaches were introduced, including time scale decomposition, sequential decision-making for beam activation, use scheduling and power allocation, and abstraction of interference into a single critical user [30].

Aditya S. Rajasekaran and Halim Yanikomeroglu in 2023, explained a computationally effective two-stage machine learning-based approach that uses neural networks to address the cluster assignment issue in a mmWave-NOMA system while taking into account the unique SIC decoding abilities of each user. To allocate users to clusters in real time, the artificial neural network (ANN) uses the instantaneous CSI and SIC decoding capabilities of each user as inputs [31].

In 2023, Waheed M. Audu and Olutayo O. Oyerinde presented joint power allocation (PA) and power splitting (PS) optimization for simultaneous wireless information decoding and energy harvesting (SWIDEH) with a modified user grouping and HP design. By changing a fixed initial correlation threshold into a function of changing discovered influencing parameters, an adaptive initial threshold-based cluster head selection strategy is presented. This enhances the analogous channel, correlation-based user grouping, and

quantized analog precoder for a ZF digital precoder design to eliminate inter-user interference [32].

In 2023, Nhat Tien Nguyen et al. used mmWave technology to study the effectiveness of a hybrid satellite-terrestrial relay system based on NOMA. The relays also have several antennas and use the AF protocol to send the information from the satellite that has been overlaid to other locations. The best relay is then selected by taking the rain coefficient into account as the mmWave band's fading factor [33].

1.3 Problem Statement

The need to move toward new techniques with higher performance and greater capacity becomes urgent to accommodate more users due to the growing number of users. Communications methods can utilize the limited spectrum resources effectively in the situation of multiple access. According to numerous research, NOMA is one of the most significant multiple access techniques that exhibit high efficiency in managing spectrum resources and high throughput.

The main problem discussed in this thesis is how to increase user fairness. In OMA, the edge user suffers from poor data rates and signal quality. NOMA fixed this problem by giving the edge user more power than the near user by employing suitable power allocation. The second problem is the limited bandwidth of the sub-6 GHz frequency bands for a single carrier. One solution to this issue is to use mmWave technology. The fourth generation (4G) and 5G networks have made extensive use of sub-6 GHz frequency bands, which are normally employed for cellular communication. However, more bandwidth is needed because of the rising demand for higher data rates and more capacity. The third issue considered in this thesis is beamforming techniques. The latter plays a vital role in reducing interference and enhancing the signals in the direction of the intended user. The three topics, which are NOMA, mmWave, and beamforming, are merged in this study for the sake of enhancing the SNR for the near user and signal-to-interference-plus-noise ratio (SINR) for the far user from the BS by allocating more power for the far user which will be explained later in chapter three and chapter four.

1.4 Aims and Objectives of the Study

This thesis aims to investigate different methods and techniques to enhance the performance of multi-user systems in the next generation of wireless communications. For serving several users with high-quality service, the MIMO-NOMA system is proposed to work over the new uncongested mmWave band. Several issues are considered to tackle issues inherent in the proposed system as listed below:

1. The pairing algorithm is used and applied for user clustering, in which two users in each cluster are served via NOMA depending on their channel circumstances.

2. SIC is used to remove the interference caused by the superposed signal of NOMA for the two users in a cluster.

3. To tackle the inherent path-loss of mmWave frequencies, cooperative decode-and-forward (DF) relaying is used and applied for the sake of performance enhancement.

4. For massive MIMO transmissions, digital beamforming is investigated and employed to increase the signal of the interest direction and reduce the interference, which consequently, enhances the SINR

5. Two beamforming techniques are considered and designed for the proposed system, i.e. ZF beamforming and maximum ratio transmission (MRT) beamforming.

1.5 Thesis layout

This thesis consists of five chapters: The introduction, and literature review presented in chapter one. The theoretical background of NOMA, mmWave, and other techniques that are used with them, such as massive MIMO and beamforming illustrated in chapter two. In Chapter Three, cooperative relays in a DF mode are utilized with the proposed NOMA-MIMO system over mmWave bands to tackle the attenuation caused by the path-loss of mmWave bands. Additionally, a combination of Sub-6 GHz and mmWave bands are suggested for backhaul and access links, respectively, in which NOMA is exploited in the backhaul link while conventional OMA is employed in the access link. In Chapter Four, Massive MIMO with NOMA is considered to serve multiple users over mmWave channels, and a BS with tens of antennas is proposed to provide services to users in the coverage area by applying beamforming techniques. Conclusion and future works suggestions are presented in Chapter Five.

CHAPTER TWO

THEORETICAL BACKGROUND

2.1 Non-orthogonal Multiple Access

As opposed to traditional OMA schemes, NOMA encourages multiple users to transmit simultaneously by utilizing the same code, and over the same frequency, but with different levels of power [9]. NOMA has two major categories; power domain and code domain, in this study NOMA power domain is proposed. In the power domain, users with better channel conditions, are given less power depending on NOMA theory, and by using SIC [34], these users can decode their data. Hence, these users will be aware of the signals corresponding to other users. This prior information can be used to improve performance, but it was not taken into account in previous forms of NOMA [10]. To effectively utilize the historical information included in NOMA systems, a cooperative NOMA transmission scheme is presented in this study [12]. The sequential detection approach is used at the receivers, in particular, since users with higher channel gain must detect and decode signals of other users with weak channel conditions, by using the SIC strategy at their terminals; the users with good channel conditions can be utilized as repeaters, i.e., relays, to enhance the reliability of the received signals of the users with weak channel gains with the service provider. Messages can be sent from users with better channel conditions to those with worse channel conditions by employing short-range local communication techniques like ultra-wideband and Bluetooth. These analytical outcomes show that the largest diversity gain for all users can be obtained via NOMA. The outage probability and diversity order attained by this cooperative NOMA scheme are examined. Due to the difficulty of coordinating user participation, requesting all users under the coverage of a NOMA network to be engaged may not be feasible in practice.

Moreover, grouping users with high channel quality does not always result in a significant performance improvement over OMA, hence the technique of user pairing can be a promising approach for the minimization of systems' complexity [35]. Instead, it is preferred to connect users who have more distinct channel profiles, i.e., they show a significant difference in channel gains due to different distances and attenuation conditions [36].

Figure 2.1 illustrates the basic difference between NOMA and OMA, where NOMA allows multiple users to use the same resources of time-frequency with different levels of power, on the other hand, OMA only allows each user to use the allotted resources of time-frequency.
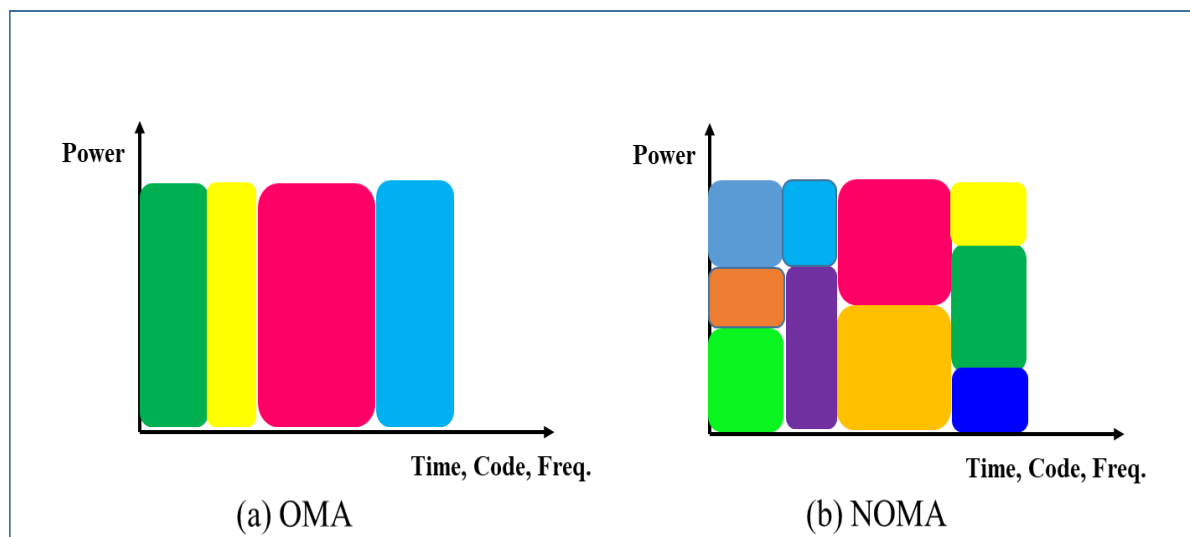
Figure 2.1: The difference between OMA and NOMA [37].

2.1.1 Successive Interference Cancellation

The severe multiple-access interference seen in NOMA systems, which is brought on by users sharing the same spectrum, is a distinctive characteristic of these systems. It has been demonstrated that the technique of SIC is efficient in reducing this interference. The overlapped signals' varying power levels are one of the requirements for a successful SIC. Additionally, the SIC method

reconstructs the signal with the greater level of power in the first step and subtracts it from the full received signal to produce the next-order signal with the lower power allocation factor (PAF) [16], and so on. By employing this method, the SIC eliminates interferences brought on by signal overlap in the power domain iteratively, by identifying and removing the signal of higher-order power until the signal of interest is identified [38]. The perfect SIC is proposed in this study.
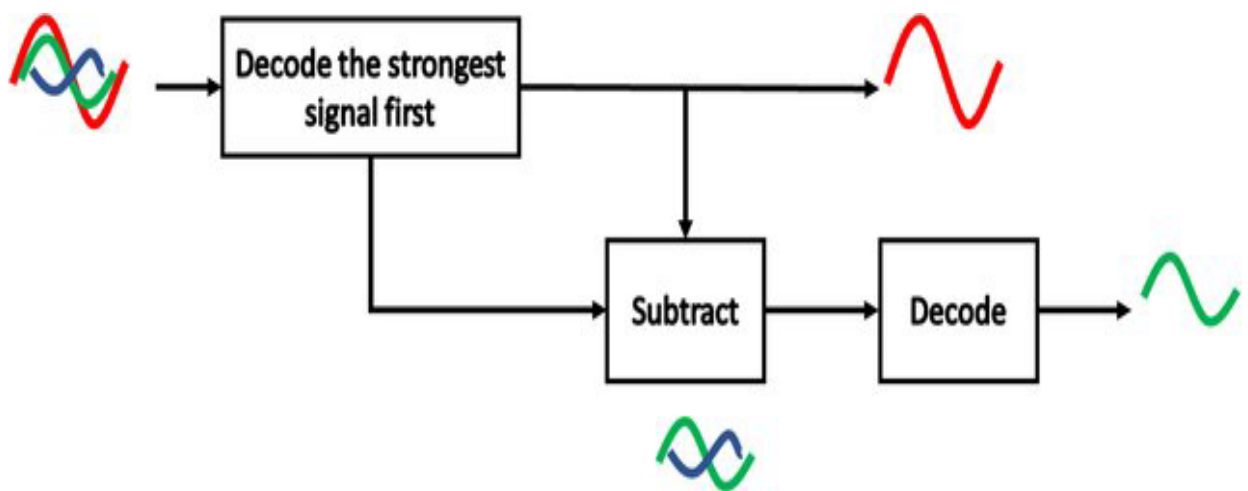
Figure 2.2: Successive interference cancellation technique [39].

2.1.2 Power Allocation (PA)

Given that users are multiplexed in the power domain, PA is essential in NOMA. As with the management of interference, user admission, and rate distribution, it has an immediate impact on the system's performance. An ineffective PA may result in a system outage because of SIC failure as well as an unjust rate allocation among users. Users' channel circumstances, CSI availability, quality of service (QoS) requirements, total power constraint, the system aims, and other factors need to be taken into account while creating PA strategies. A few often-used PA performance parameters are the number

of admitted users, energy efficiency, sum rate, outage probability, user fairness, and total power usage. As a result, the objective of PA in NOMA is to achieve either increased numbers of permitted users, a greater energy efficiency, and sum rate, or balanced fairness with minimal power usage [40].

2.1.3 Superposition Coding

Superposition coding (SC) is a technique used with NOMA. It is represented the sum of the multiuser signals at the transmitter, each user receives the SC signal and decodes its signal, whereas the far user with bad channel gain decodes its signal and treats other signals as interference, on the other hand, the near user with good channel gain subtracts the far user signal from the SC signal and decode its signal by using SIC [41].

2.1.4 Channel Capacity

The maximum rate at which data may be transmitted through a channel is known as the channel capacity it is measured in bits per second (bps) according to Shannon's theorem which can be written as [42]:

$$C = Blog_2(1 + SNR) \tag{2.1}$$

where C is the channel capacity, B is the bandwidth of the passband system in (Hz), and SNR represented the signal-to-noise ratio, by adding the effect of user's interference the SNR changed to the SINR.

2.1.5 Spectral Efficiency

The amount of data that can be sent over a specific bandwidth (BW) or frequency range in a communication system is referred to as spectral efficiency. In other terms, it is a measurement of how effectively a communication system transmits data using the available frequency spectrum. Spectral efficiency in wireless communication is commonly expressed as bits per second per Hz (bps/Hz). More bits of data may be sent per unit of frequency BW as spectral efficiency increases.

$$\text{SE} = \frac{Data\ Rate(bps)}{System\ BW(Hz)} \quad \text{(bps/Hz)} \tag{2.2}$$

There are many ways to boost spectral efficiency, including modulation systems that can transport more bits per symbol and use numerous antennas to increase spatial variety [43].

Since NOMA serves several users in the same resource block, it often has a higher spectral efficiency than OMA. NOMA achieves this by allocating varying power levels to users based on their channel circumstances, maximizing the utilization of available bandwidth. Contrarily, OMA allots orthogonal resources to every user, which might result in underutilization of the spectrum, particularly in situations where users' channel conditions are varied. Figure 2.3 shows the spectral efficiency comparison between NOMA and OMA.
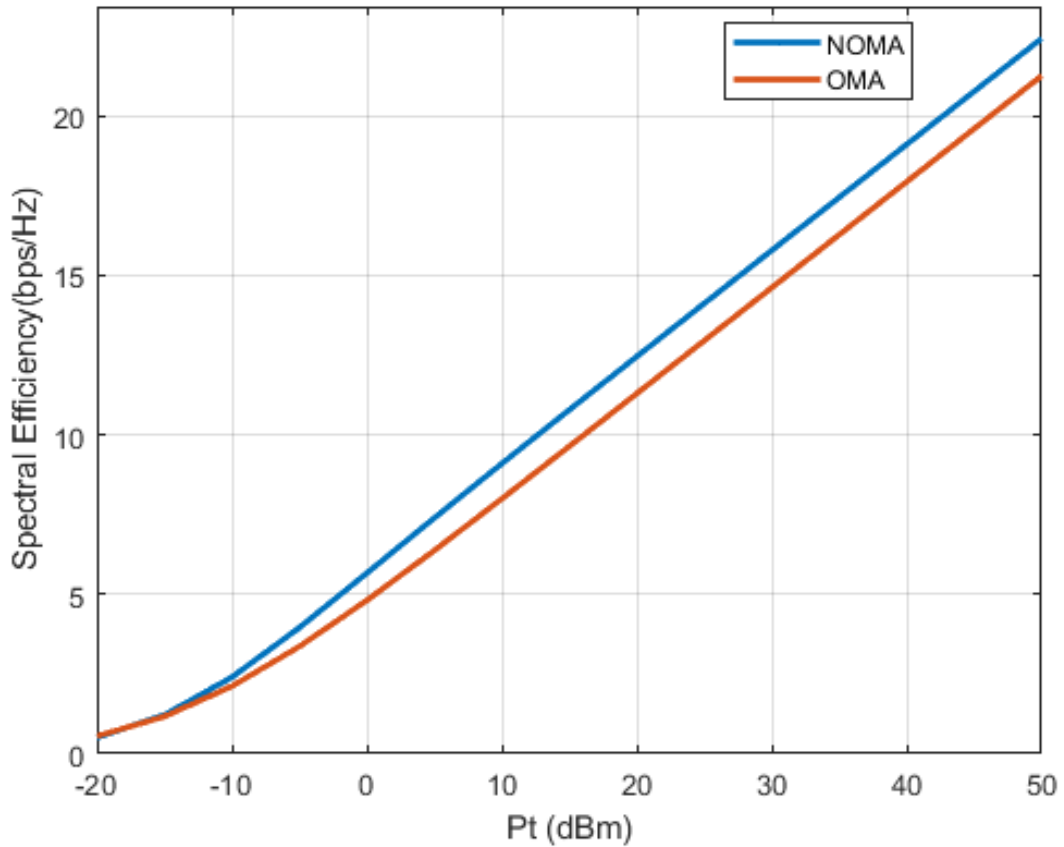
Figure 2.3: Spectral efficiency comparison between NOMA and OMA for 2x2 MIMO system.

2.1.6 System Throughput

The quantity of information, tasks, or data that a system can process in a specific length of time is referred to as system throughput. Often defined in terms of bits per second, it is a measurement of the system's capacity to process or send information. A system that can process more data and complete more tasks in less time will often have a greater throughput. It is a crucial performance indicator for systems that need to process a lot of data. Depending on the system type, many factors may influence throughput. The throughput of a computer system can be affected by several variables, including the consumed power in the center processing unit, memory speed,

the effectiveness of the software algorithms, and the storage devices' capacity. In a network system, elements like the network connection's capacity, the effectiveness of the network protocols, and the networking devices' computing power can all affect the system's throughput [44].

2.1.7 Outage Probability

The probability that a communication system or network will not achieve a specific performance standard, such as a minimum data rate or a maximum error rate, under a given set of environmental factors is known as outage probability. In other words, it is the probability that a certain set of conditions will not result in the proper operation of the system or network [45]. To analyze the outage probability, it has been considered the threshold communication rate for each user. Let us denote the threshold rate for U_1 as r_1 and the threshold rate for U_2 as r_2. The outage event occurs when either U_1 or U_2 fails to obtain their respective threshold rates. The outage probability of the far user P_{out1} can be directly defined as the probability that the data rate falls below the target rate, which can be expressed as:

$$P_{out1} = P_r(\log_2(1 + \gamma_1) < r_1) \tag{2.3}$$

On the other hand, at the near user, i.e. U_2, SIC is performed to cancel the interference caused by the far user, U_1, which makes the outage probabilities rely on the accuracy of this process.
As a result, by assuming the perfect SIC process at U_2, its outage probability can be expressed as:

$$Pout2 = P_r(\log_2(1 + \Omega_2) < r_2) \tag{2.4}$$

2.1.8 Downlink NOMA

In a downlink NOMA transmission, the BS will schedule k users to use the same spectrum resources. Assume additionally that the message signal for i_{th} user is s_i, where $E[|s_i|^2] = 1$, and transmit power is p_i. The superposed signal at the transmitter end can be written as [46]:

$$X = \sum_{i=1}^{k} \sqrt{p_i s_i} , \qquad\qquad (2.5)$$

where $\sum_{i=1}^{k} p_i \leq p_t$, for BS total transmit power budget of p_t. On the other hand, at i_{th} user end the received signal can be written as [46]:

$$y_i = h_i X + n_i \qquad\qquad (2.6)$$

where h_i represented the gain of the complex channel between BS and the user i, and n_i is the receiver Gaussian noise including the inter-cell interference at the i_{th} user's receiver with power spectral density $N_{f,i}$.

A simple NOMA system with two users and a single BS is presented in Fig.2.4
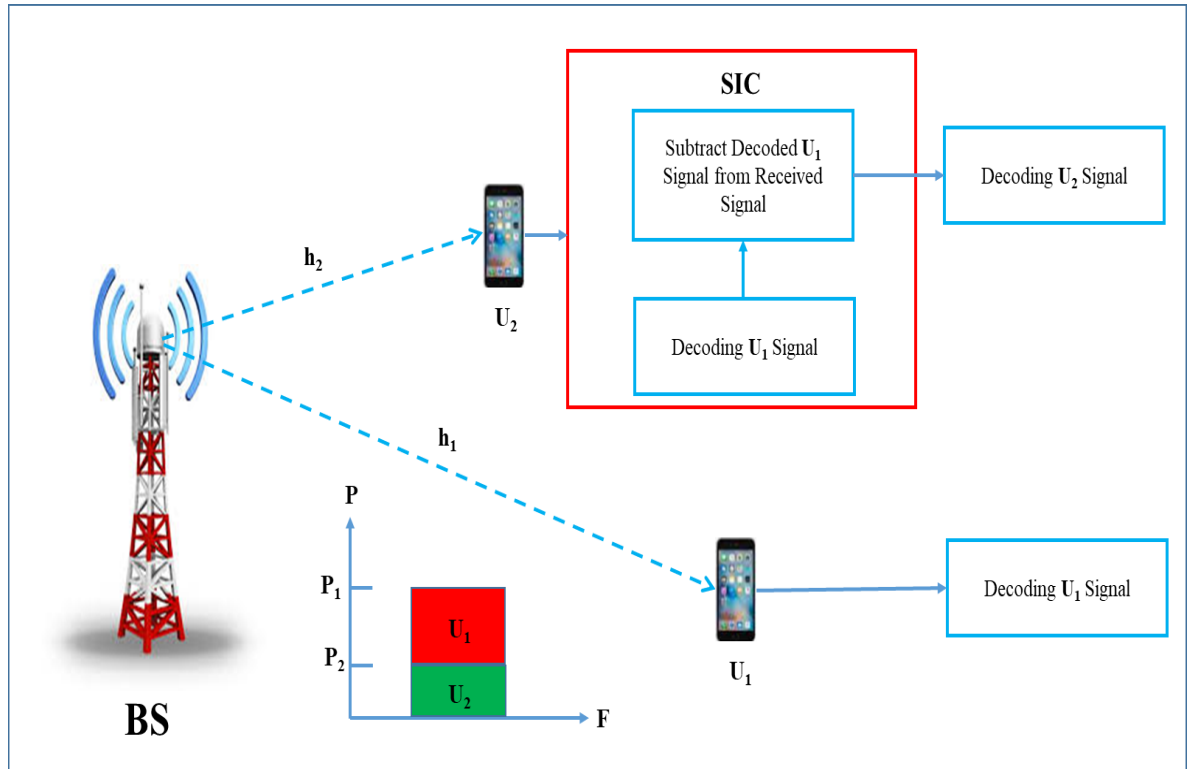
Figure 2.4: Two-user downlink NOMA

At the receivers, SIC is used to separate the signals from various users. According to $|h_i|^2/N_{f,i}$. The best order for SIC decoding is in decreasing order of the users' channels' strengths. Each user can effectively eliminate interference from the signals of other users whose decoding commands occur after them using this order. As a result, user 2 (with the strong channel) $|h_2|^2/N_{f,2}$, can cancel out interference from user 1 (with the weak channel) $|h_1|^2/N_{f,1}$. It is crucial to remember that the BS regularly orders SICs based on CSI feedback from users and that the BS provides users with the latest information on SIC ordering. Without losing generality, it can be said that to improve the SINR, a user with a weak channel is given high power than a user with a strong channel. For the two-user NOMA with $|h_2|^2/N_{f,2}>|h_1|^2/N_{f,1}$ ($P_2<P_1$), only user 2 used SIC. It decodes s_1 first, the user 1 signal, and then remove it from the signal received y_2, after that, it decodes its signal. User 1 treats the user 2 signal s_2, as noise and so directly decodes its signal from y_1 without using SIC. If SIC is perfect, the NOMA user i achievable data rate, R_i^{NOMA} for a transmission, with 1 Hz BW can be expressed as [40]

$$R_1^{NOMA} = \log_2\left(1 + \frac{P_1\,|h_1|^2}{P_2|h_1|^2+N_{f,1}}\right). \qquad (2.7)$$

$$R_2^{NOMA} = \log_2\left(1 + \frac{P_2\,|h_2|^2}{N_{f,2}}\right). \qquad (2.8)$$

The sum capacity that can be reached is $R^{NOMA} = R_1^{NOMA} + R_2^{NOMA}$. According to equations (2.5) and (2.6), the BS can regulate each user's data rate by adjusting the power allocation coefficients α_1 and α_2, where $\alpha_1=\frac{P_1}{P}$ and $\alpha_2=\frac{P_2}{P}$ [40].

2.1.9 Advantages of NOMA

Many advantages of NOMA are summarized below:

- **Increased Spectral Efficiency**: In comparison to OMA schemes, NOMA provides better spectral efficiency. The capacity of the system can be increased by NOMA by allowing several users to share the same time and frequency resources. As a result, the spectrum is used more effectively, and the system as a whole performs better.

- **Low Latency:** As simultaneous transmissions and receptions are possible with NOMA, latency is decreased. Users can send and receive data at the same time slot, reducing waiting periods and enhancing system responsiveness overall.

- **Energy Efficiency:** The communication system's power consumption can be decreased with NOMA to increase energy efficiency. NOMA minimizes the need for extra frequencies and time slots, which in turn results in less power usage by allowing several users to share the same resources.

- **Improved User Fairness:** Resource allocation among users is made more egalitarian by NOMA. With NOMA, each user is given a variable power level, with users with weaker channel conditions receiving greater power allocations than with OMA schemes, which distribute resources equally among users. By doing this, regardless of the channel quality, it is made sure that every user has an equal opportunity to access the system's resources.

- **Enhanced Coverage:** Wireless communication systems' coverage areas can be expanded with NOMA. NOMA can reduce interference and improve the signal quality for users near the cell edge or in poor channel circumstances by allowing numerous users to share the same

resources. In regions with difficult propagation circumstances, this results in higher coverage and a better user experience.

- **Enhanced Connectivity:** For users at the cell edge, NOMA can offer improved connectivity. OMA methods frequently result in performance degradation for cell-edge users as a result of scarce resources and interference from nearby cells. Cell-edge customers are given higher priority and improved connectivity because of NOMA's more effective resource distribution.

2.1.10 Drawbacks of NOMA

There are some of NOMA drawbacks [47] which can be listed as:

- **Complexity in the receiver**: Each user in the cluster is required to decode the information of every other user, even the one with the weakest channel gains. The receiver becomes more complex as a result. Additionally, energy consumption has increased.

- **Limitation in maximum number of users:** All of the other users' information will be incorrectly decoded if a single user has SIC error. This restricts the maximum number of users that each of the cell's clusters can serve.

- **Sensitivity of the system:** Because each user needs to send feedback to the base station about their channel gain, NOMA is sensitive enough to measure these parameters.

2.2 Millimeter Wave Spectrum

The huge demand for mobile multimedia services and for accessing data at anytime and anywhere forced telecommunications companies to reconsider how cellular networks are built. Wireless businesses have developed a new 5G standard to satisfy this demand. Over the past few years, interest in

research on next-generation 5G wireless systems, which aspires to address multiple unprecedented technical requirements and obstacles, has grown in both academia and industry. It is possible to consider increasing the efficiency of the energy and spectrum of the current generation network, i.e. the 4G, in which the bands in the range (0.6-3) GHz are essentially congested, to satisfy the 5G criteria. Studies indicate that this gain will not be enough to support the 5G network's capacity. Due to the vast amount of accessible bandwidth, mmWave frequency ranges between 30 and 300 GHz have drawn a lot of attention regarding addressing the capacity requirements of 5G networks. Although mmWave frequencies have a very wide range of usable BW [48], their propagation properties differ greatly compared to sub-6 GHz and microwave. Theoretically, mmWave frequencies range from 30 to 300 GHz, or from 1 to 10 mm in wavelength. However, mmWave bands are the name given by wireless researchers to frequency ranges over 6 GHz [14].

Figure 2.5 illustrates how the mmWave signals are shorter than radio waves or microwaves but slightly longer than X-rays or infrared radiation. Based on comprehensive measurements made for the 28 GHz, 38 GHz, 60 GHz, and 73 GHz frequency bands.
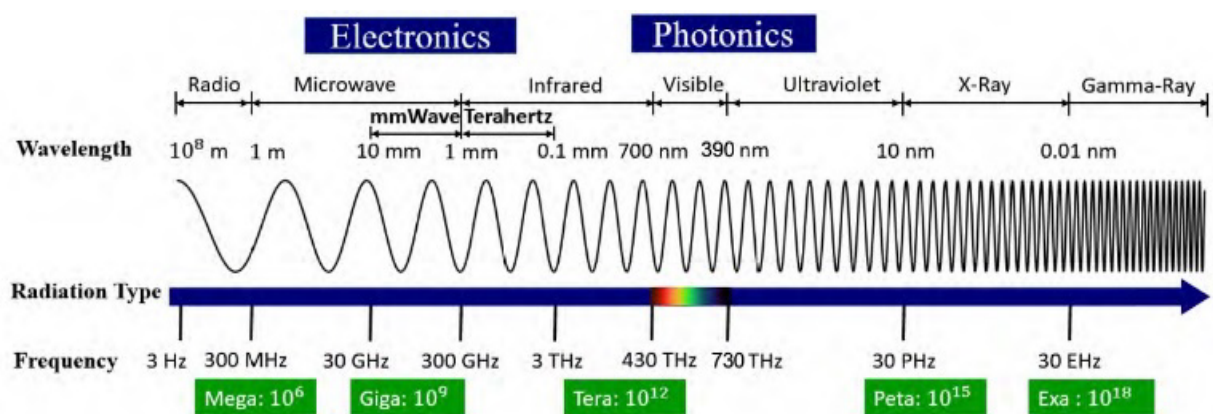
Figure 2.5: The electromagnetic spectrum [48].

2.2.1 Millimeter Wave Propagation Characteristics

The propagation characteristics of the mmWave band are different from those of normal lower frequency band communication networks, involving more modeling and design work for communication systems, the size of wireless links, as well as their power needs.

The main propagation characteristics of mmWaves are explained in Fig.2.6 [49], including atmospheric attenuation, free-space path loss, material penetration, Doppler effect, foliage attenuation, rain-induced fading, propagation mechanisms (multipath, reflection, scattering, diffraction, refraction). Only the free-space path loss discussed in this study.
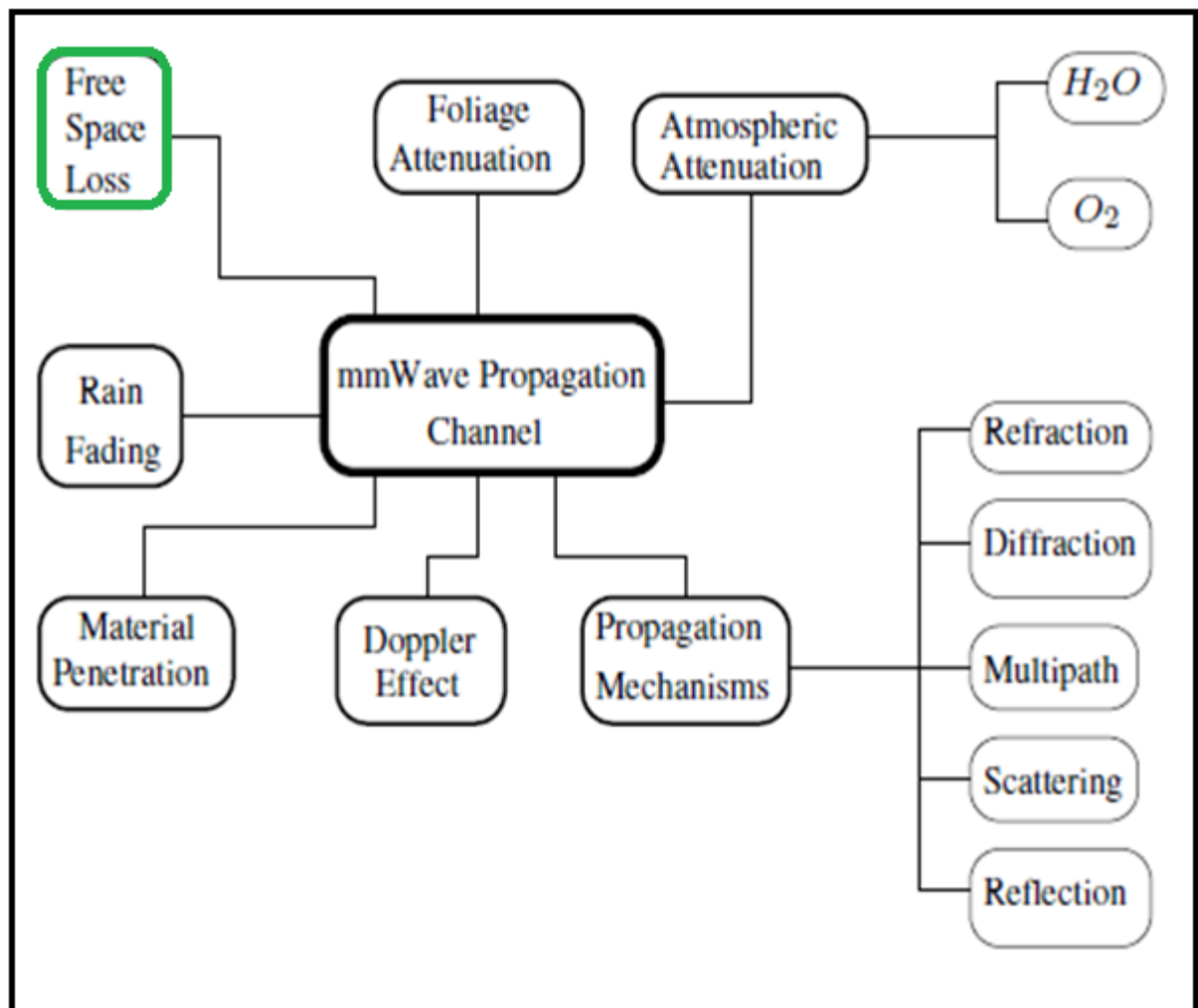
Figure 2.6: Propagation characteristics of mmWave [49]

2.2.2 Free Space Path Loss

Free space path loss (FSPL) is defined as the loss in signal strength of an electromagnetic wave between the transmitter and receiver of the communication system through free space which can be expressed in decibel scale as [50]:

$$FSPL = 92.4 + 20 \log f + 10 \log d , \qquad (2.9)$$

where d is the distance between the transmitter and receiver in km, f is the carrier frequency in GHz.

The FSPL is not the only environmental component that affects the propagation of the mmWave signal. Other environmental parameters, such as atmospheric absorption by gases like oxygen and water vapor, and rainfall, are also very important as shown in Fig.2.7 [49].
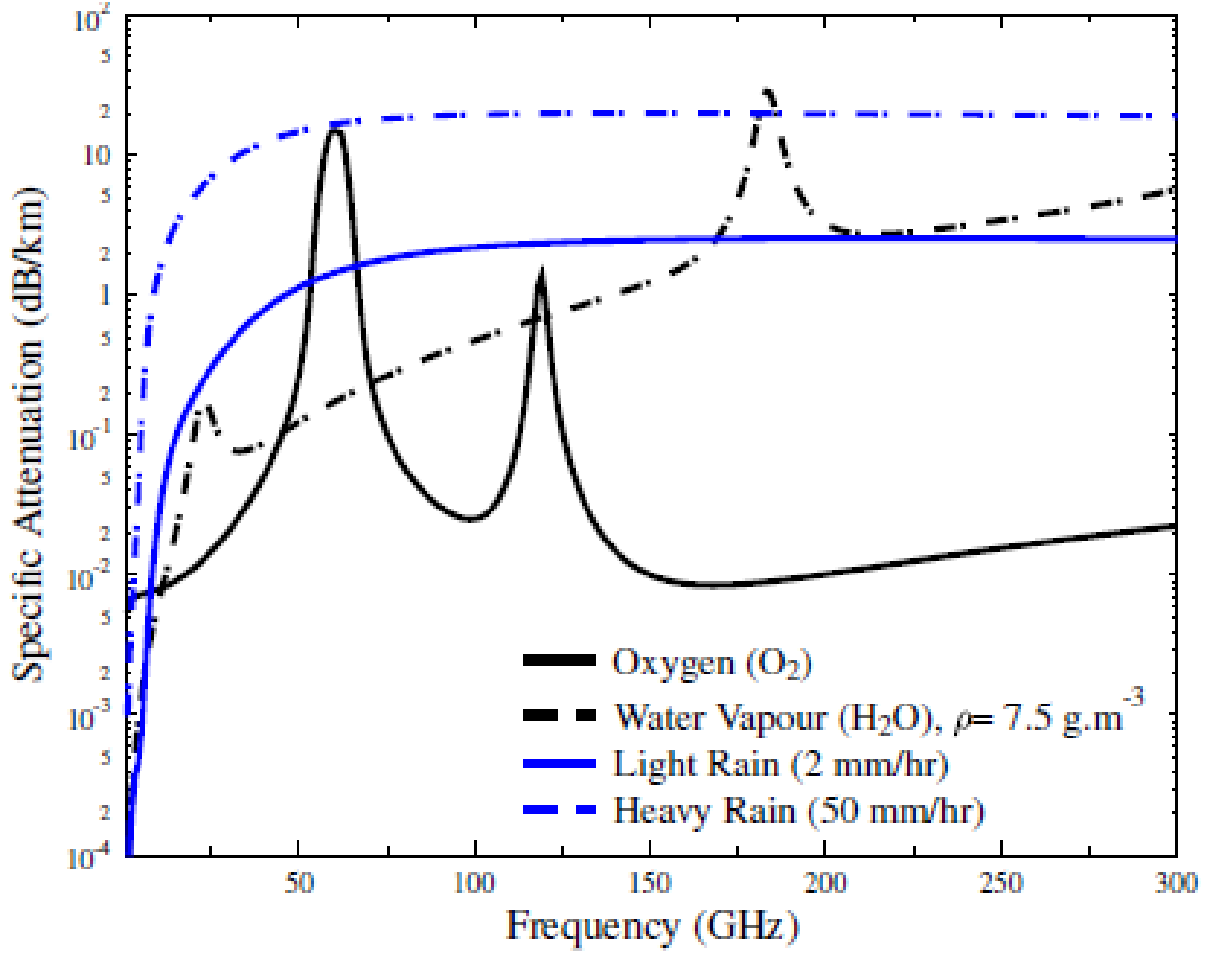
Figure 2.7: Specific attenuation curves of O2, H2O, and rain at sea level.
The term ρ refers to the density of H_2O in $grams$ per $meter^3$ [49]

There are various types of path loss models. Some of them include the close-in free space reference distance (CI) model, the floating intercept (FI) model, the dual-slope model [14], and the parabolic model, only the first and second models would be discussed in this study.

CI path loss model can be expressed as [49]

$$PL^{CI} [dB] = FSPL + 10\,n\,log\left(\frac{d}{d_0}\right) + X_\sigma^{CI}, \qquad (2.10)$$

where $d_0 = 1m, d \geq d_0$, n is the path loss exponent, X_σ^{CI} is a zero-mean Gaussian random variable with σ as the standard deviation in (dB).

On the other hand, the FI path loss model can be expressed as [49]

$$PL^{FI}\ [dB] = \ \delta + 10\ \beta\ log\ \left(\frac{d}{d_0}\right) + X_\sigma^{FI}, \qquad\qquad (2.11)$$

where δ is the FI coefficient in dB, β represented the line slope, and σ is the standard deviation of the linear fit line.

2.2.3 Cooperative Communication

Cooperative communication performance has been thoroughly investigated for various relaying protocols, system topologies, and system parameters. It has been specifically determined how well AF and DF relay networks perform for various fading channels in terms of diversity gain, capacity, bit error rate (BER), and outage probability [51]. To estimate the transmitted signals in networks with several relays, the destination must first combine the received signals. The maximum signals received from many routes have regularly been combined using ratio combining.

2.3 Multiple Input Multiple Output

Due to the enormous number of subscribers, wireless communication is being used more frequently, which has increased the need for methods to meet the rising demand for high data speeds with acceptable outage probabilities and low BER. These requirements can be satisfied by the MIMO technology, which uses multiple antennas at the transmitter and multiple antennas at the receiver. Through the use of spatial multiplexing, or multi-path transmission, which involves data being sent simultaneously from all transmitter antennas by uncorrelated channels to all receiver antennas via various paths, MIMO significantly increases gain diversity. As a result, the data rate is greatly increased and the BER is significantly decreased. Multiple copies of the signal that arrive at the receiver assure a positive combination of the sent signal [52].

Figure. 2.8, shows the MIMO technique between the BS with the users.
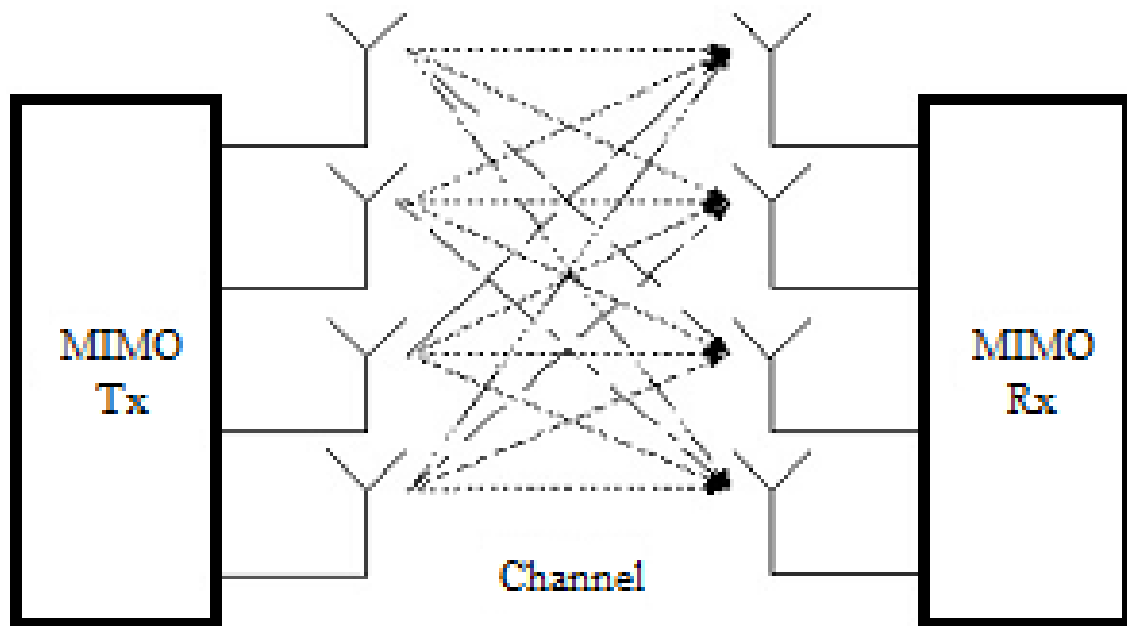
Figure 2.8: MIMO system[53].

When the BS uses a large number of antennas the new system is called massive MIMO.

Massive MIMO is generally understood to be a physical layer technology that provides each BS with a sizable number of active antennas which can be used to spatially multiplex numerous users to communicate with them on the same time and frequency resource. By using spatial signal processing methods like receive combining and transmit precoding to deal with signal attenuation and interference, spectral efficiency per cell can be increased by orders of magnitude over traditional cellular networks. In summary, massive MIMO pushes spatial multiplexing to the limit by upgrading the Space-Division Multiple Access (SDMA) protocols.

The main advantages of massive MIMO systems are high energy efficiency, reliable communications, huge spectral efficiency, favorable propagation, low complexity signal processing, and channel hardening [54].

In Massive MIMO, the base station is equipped with hundreds or even thousands of antennas, which are utilized to produce many beams that may be aimed at specific users. The base station can simultaneously serve numerous users with large data rates, decreased latency, and improved spectral efficiency [55].

Massive MIMO has the potential to transform wireless communication, particularly in the context of 5G networks and beyond. While utilizing less power and spectrum, it provides larger capacity and improved dependability. [56].

2.4 Beamforming

Beamforming is a signal processing method used in wireless communication networks to enhance system performance by directing the signal's transmission or reception in a particular direction. The method is based on concentrating the signal in the receiver's direction using several antennas, which reduces interference and improves the SNR. To enhance the performance of wireless communication systems, beamforming, and NOMA have been suggested as a combination. The system's spectral efficiency can be raised via beamforming, which focuses the signal in the direction of the intended user, and NOMA, which allows several users to use the same resource block [57] [58]. Figure 2.9 shows, in general, how the BS creates beams for several users depending on their locations and channels circumstances. There are several types of beamforming such as: analog beamforming, digital beamforming, and hybrid beamforming.
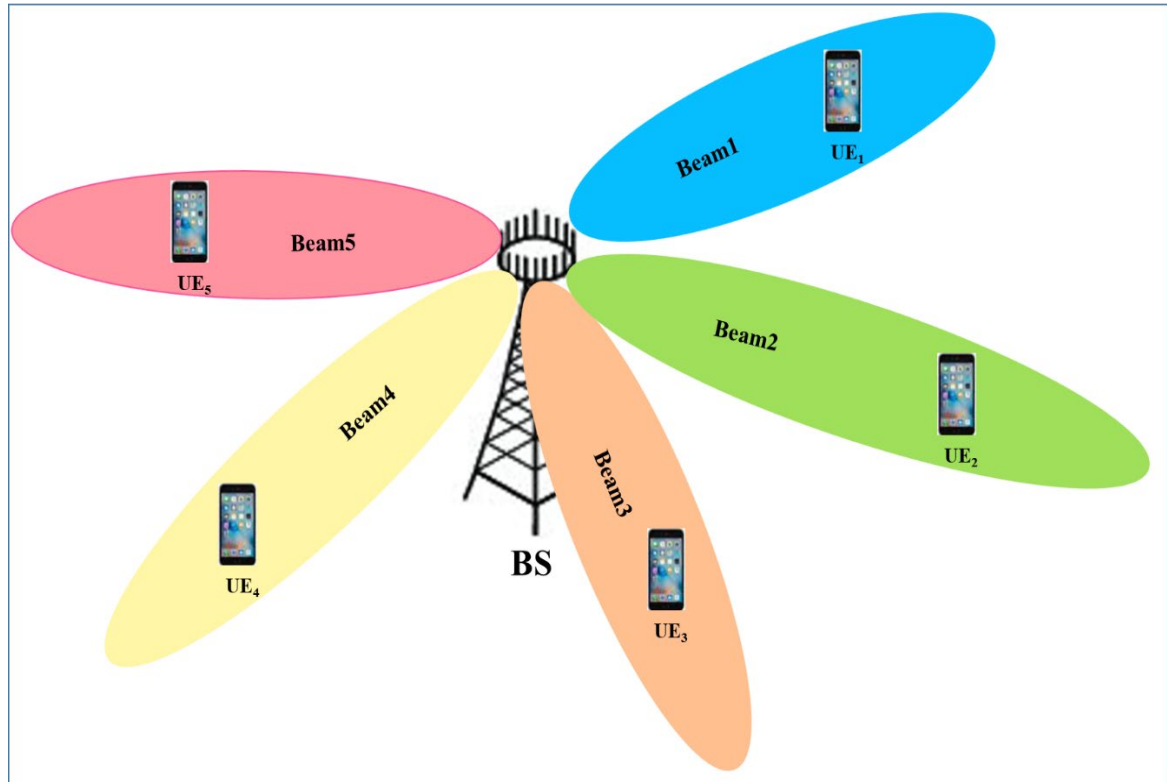
Figure 2.9: Beamforming with massive MIMO antenna [57].

2.4.1 Advantages of Beamforming

The advantages of beamforming can be listed as:

- **Increased Range and Coverage:** In comparison to conventional omnidirectional antennas, beamforming offers greater range and coverage. Beamforming increases the range of wireless communication systems and permits communication over greater distances by concentrating the transmitted energy in a particular direction. This is especially helpful in situations where signals need to be sent over long distances or in environments with obstacles or interference [59].

- **Improved Signal Quality:** Beamforming minimizes the effects of background noise and multipath interference by directing the sent or received signals toward the desired target or receiver. As a result, the

total system performance is increased along with the signal quality and signal degradation [60].

- **Increased Capacity and Spectral Efficiency:** Beamforming techniques can be used in wireless communication networks to target particular users or objects with signals. As a result, the frequency spectrum can be used spatially by several users or devices to transmit and receive signals at the same time, boosting system capacity and spectral efficiency [59].

- **Reduced Power Consumption:** Beamforming reduces the energy lost in other directions by concentrating the transmitted energy towards the intended target. Reduced power usage is the result, which is significant for systems that are energy-constrained and use batteries [60].

- **Privacy and Security:** Beamforming enables more targeted and directed signal transmission, which lowers the possibility of listening in or intercepting. By reducing the chance that signals would reach undesired recipients, it improves privacy and security [60].

- **Compatibility with Multiple Antennas:** MIMO systems and other multi-antenna systems are good candidates for beamforming. It takes advantage of the spatial dimension to boost wireless connection quality, increase system capacity, and strengthen link reliability [61].

- **Flexibility and Adaptability:** Techniques for beamforming can dynamically adjust to shifting environmental factors such as: shifting interference levels, multipath propagation, and user mobility. To improve system performance and keep reliable communication links, adaptive beamforming algorithms can change the beam's direction and shape in real time [59].

2.4.2 Drawbacks of Beamforming

Following is some of Beamforming Drawbacks [62]:

- **Hardware complexity:** Due to the utilization of many antennas and other hardware systems, hardware complexity has increased.
- **High cost:** The cost of a beamforming system is more expensive than a non-beamforming system due to increased hardware resources and the use of powerful digital signal processing chips.
- **High signal processing:** Because mathematical techniques were used in the construction of the beamforming system, a high-performance digital signal processor is required.

2.4.3 Analog Beamforming

In this architectural scheme, an analog beamformer is constructed using one RF chain which is consist of many electronic components such as mixer, amplifier, bridge, etc, and several shifters distributed over the antenna elements. The phases of each antenna signal are changed in the RF domain. The antenna gain increase that analog beamforming provides partially mitigates the effect of high path loss in mmWave by altering the pattern of radiation and the performance of antenna arrays. An Analog beamformer with one RF chain is shown in Fig.2.10 [57].
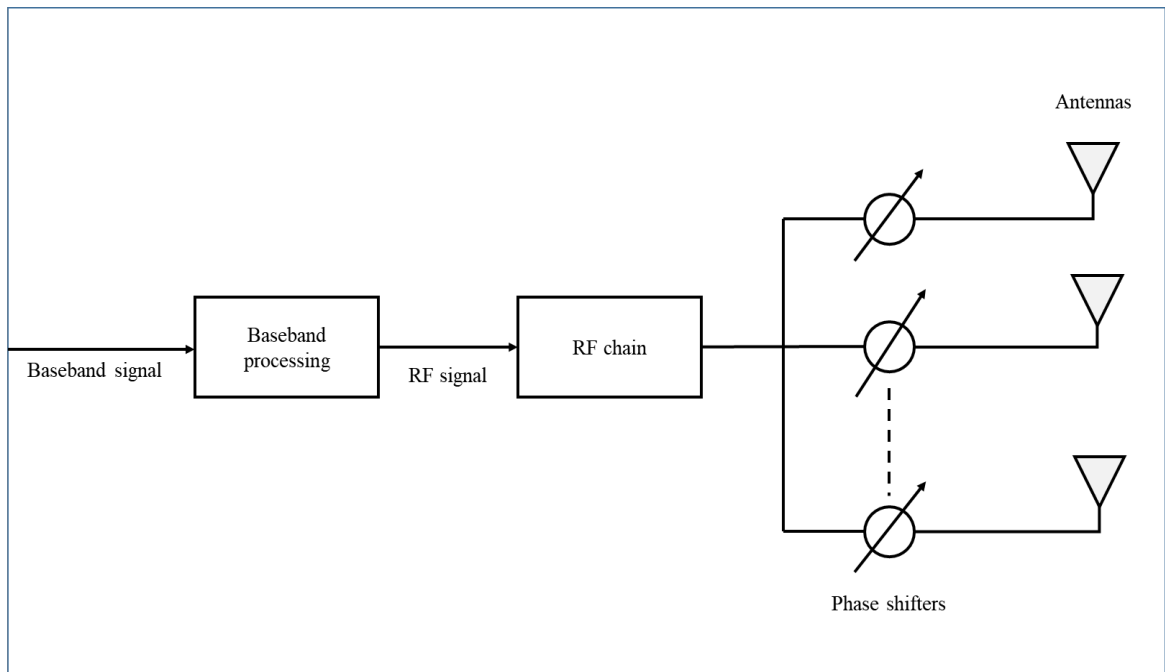
Figure 2.10: Analog beamforming basic diagram

2.4.4 Digital Beamforming

Baseband beamforming or precoding are two ways to explain digital beamforming. In the baseband processing step before RF transmission, the signal is precoded (amplitude and phase adjustments). The same group of antenna elements can simultaneously produce multiple beams, one for each user. Since numerous users can receive data from a cell concurrently using the same frequency and time resources, digital beamforming improves cell efficiency [57]. The digital beamforming structure is described in Fig.2.11.
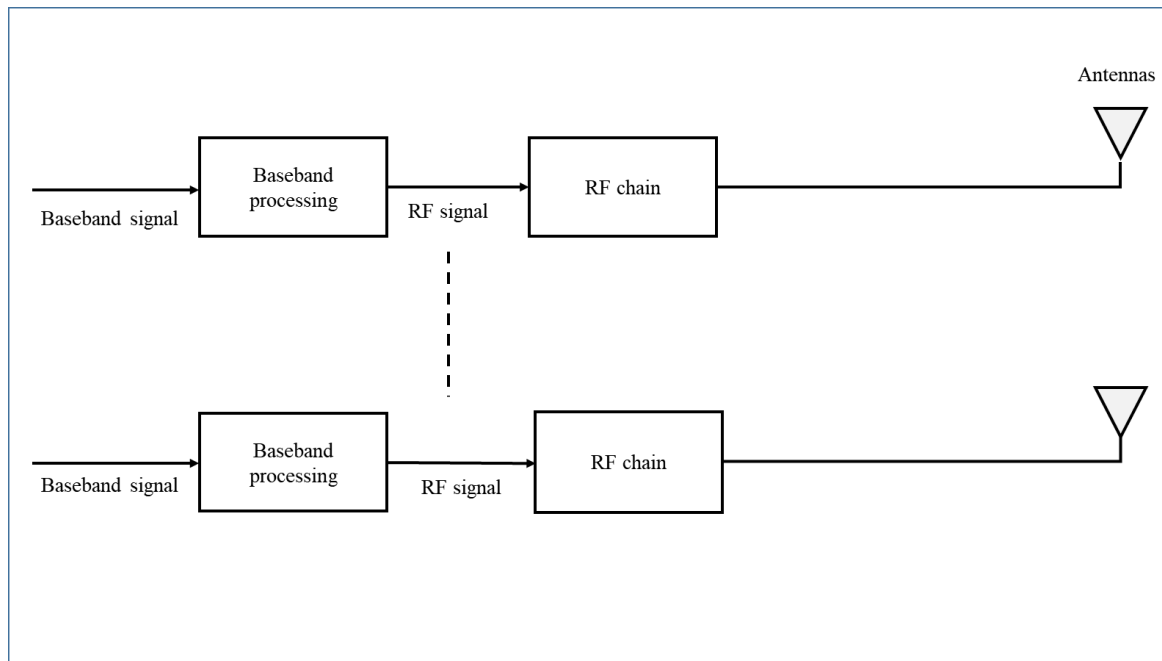
Figure 2.11: Digital beamforming basic diagram

2.4.5 Hybrid Beamforming

It combines digital and analog beamforming. It has been determined to adopt a certain type of hybrid beamforming with mmWave in 5G. The number of entire RF chains can be decreased to significantly lower costs. Additionally, less overall power is consumed as a result of this. There are fewer degrees of freedom for digital baseband processing since the number of converters is less than the number of antennas. In comparison to fully digital beamforming, the number of concurrent streams supported is thus decreased. Due to the unique channel characteristics in mmWave frequencies, the ensuing performance gap is predicted to be rather small[63]. A hybrid beamforming system with all antennas and each RF chain connected to a specific number of phase shifters is seen in Fig.2.12 [57].
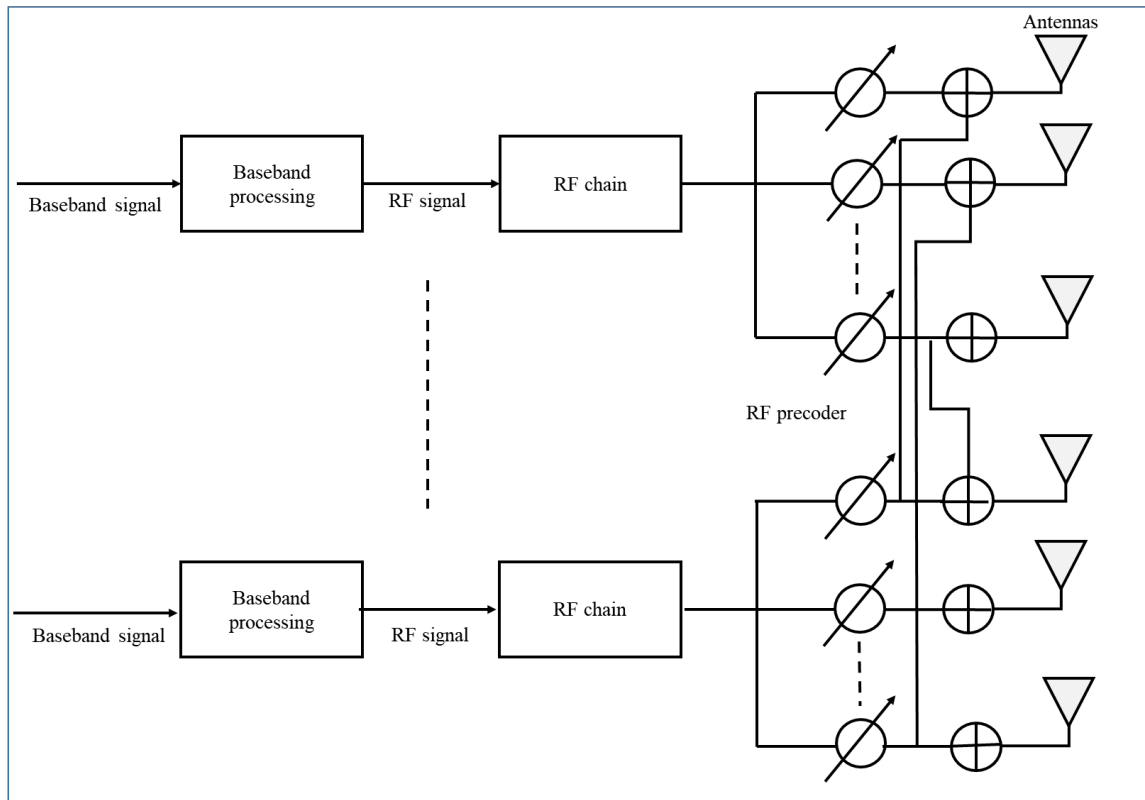
Figure 2.12: Hybrid beamforming basic diagram

Two types of digital beamforming are discussed in this study which are: ZF beamforming and MRT beamforming.

ZF beamforming is spatial signal processing for wireless devices with numerous antennas. The ZF beamforming algorithm for downlink enables a transmitter to send data to a preferred user while negating the directives of an undesirable user. In contrast, ZF beamforming receives just desirable signals for uplink while canceling out undesired signals. This method of ZF precoding is often referred to as null-steering. ZF-based precoding will improve the system's optimum capacity for a sufficient number of users when the transmitter is fully aware of the CSI of a specific downlink. Otherwise, the final output of the ZF-based precoding will exhibit reductions [64] [15].

The realization of a large order of diversity can be achieved using the transmit beamforming technique known as MRT beamforming, assuming the transmitter has the necessary side information. The effectiveness of MRT beamforming when cochannel interference is present has recently become the subject of analysis [65]. Different scenarios of NOMA beamforming are analyzed later in this thesis in Chapter Four.

CHAPTER THREE

PERFORMANCE ENHANCEMENT OF COOPERATIVE MIMO-NOMA SYSTEMS OVER SUB-6 GHZ AND MMWAVE BANDS

3.1 Introduction

In this chapter, two links with different frequency bands are considered to serve users by a BS via DF cooperative relays. Backhaul and access links are proposed with sub-6 GHz and mmWave bands, respectively. NOMA is employed in the backhaul link to transmit a superposed signal in the power domain simultaneously using the same band. The superposed signals, which contain two signals that differ in PAFs, are constructed for two selected DF relays in the BS. The two relays are chosen among several relays to be serviced by the BS via utilizing a pairing algorithm depending on different users' circumstances. The furthest DF relay detects the incoming NOMA signal directly, while the nearest one applies SIC before extracting its signal. Each DF relay forwards the detected signals toward their intended users over mmWave channels. Furthermore, three performance metrics are utilized to evaluate the system's performance, which are the outage probability, the achievable throughput, and the bit-error rate. Moreover, a comparison between two mmWave bands in the access link, which are 28GHz and 73GHz, is obtained to demonstrate the superiority of 28 GHz in the three performance metrics.

3.2 System Modeling

Without loss of generality, it has been proposed a pairing algorithm, as illustrated in algorithm 3.1, that couples an even number of relays, i.e. 2K, into K pairs. This algorithm is applied by the BS after collecting the required data regarding the CSI of all BS to relay channels, in addition to the intended rate for each user connected to a relay in the coverage area. It has been assumed that the BS is equipped with N_{tx} and N_{rx} antennas for transmitting and receiving simultaneously. The PAFs are evaluated for each relay in the created pair, depending on the required rate of the user of interest in that link.

After applying this algorithm, it focused on analyzing and evaluating the performance of one pair that contains two DF-relays, in which the BS provides NOMA services over sub6 GHz channels, and each relay delivers the BS services to an intended user with a required rate.

This system is shown in Fig.3.1, where all nodes are supplied with multiple antennas for their transmission, i.e., the system works in MIMO mode. It has been assumed N_{tx} and N_{rx} antennas for transmitting and receiving signals at each terminal, respectively. The BS transmits the signal, over a frequency non-selective Rayleigh fading channel, to the DF relay in the backhaul link, where the relay decodes and retransmits it over the mmWave channel to the terminal user. The two links work with different frequencies, in which the backhaul link employs the RF in the sub-6 GHz band, while the access link operation is in the mmWave band at 28GHz or 73GHz.
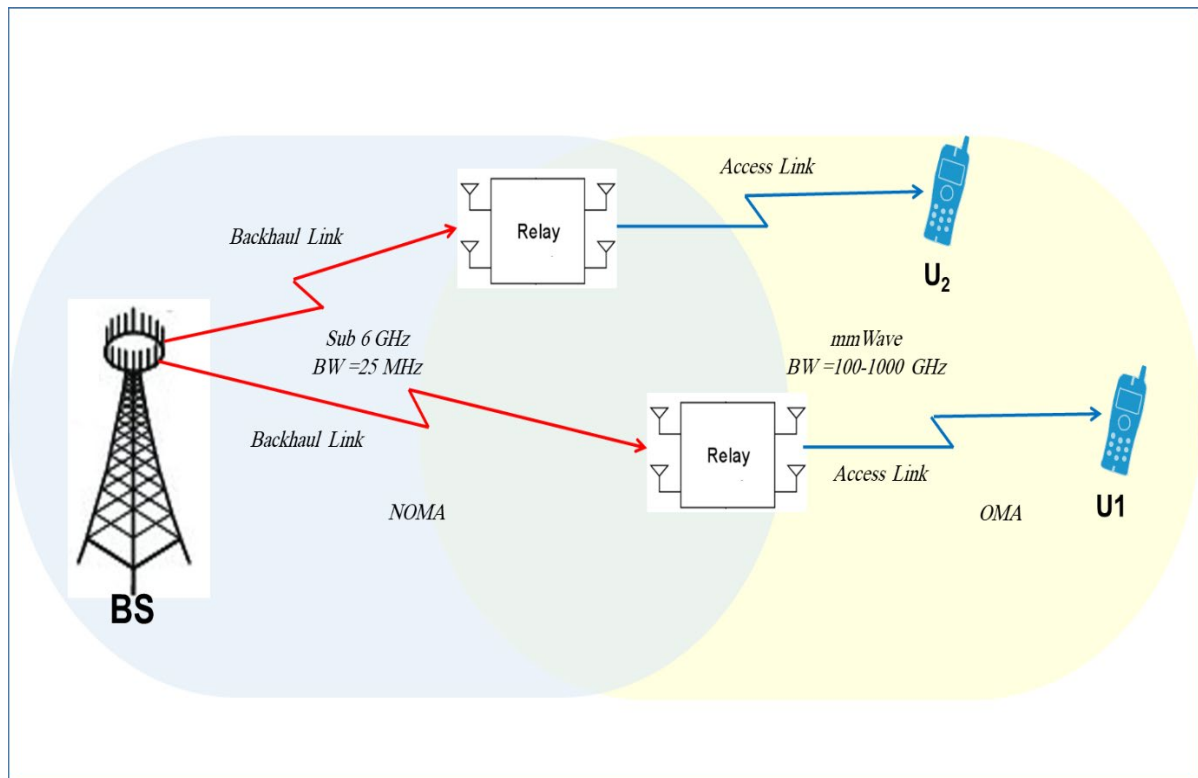
Figure 3.1: Backhaul and Access Links via DF Relays.

3.2.1 First Hop from BS to Relay (Backhaul Link)

In this section, Fig.3.1 illustrates how the BS interacts with two relays, which simultaneously use the same frequency resources while utilizing power domain multiplexing. By assigning power to each relay according to their distances away from the source, superposition coding is accomplished. When employing the PAF technique, the higher ratio of the available power is supplied to the furthest relay, and the remained power is allocated to the close one. Nevertheless, the sum of this factor for all relays must be equal to one. Since more power is allocated to the far terminal relay, the superposed power of the near relay is considered additive noise. As a result, direct detection is used at the far relay without the requirement of the SIC.

On the other hand, at the near relay terminal, the SIC process must be applied. This process includes detecting first the signal of the far relay, which

is subtracted then from the whole received NOMA signal for the near relay's signal construction. Algorithm 3.2 and Fig.3.2 explain and show the SIC process in detail. Moreover, it has been assumed flat Rayleigh fading channels, i.e. frequency non-selective channels, for the first hope of this system. Furthermore, the modulated signals for the far and near relays are denoted by x_f and x_n, respectively, and the Quadrature phase shift keying (QPSK) modulation scheme is used for all links.

In this study, the BS employs a pairing algorithm for the sake of choosing two relays among several relays in the coverage area. NOMA technique is applied on those two paired relays, where each DF relay receives, decodes, and retransmits its incoming signal to a user in the access link via the mmWave channel. PAF is applied at the BS for those two relays, the far and near relays are allocated power with $\alpha_F \, p_t$ and $\alpha_N \, p_t$, where $\alpha_F + \alpha_N = 1$, and $\alpha_F > \alpha_N$. Additionally, at the BS, the NOMA signal is created by superposing the two signals that allocated the suitable PAF for each of them. This process can be expressed as:

$$x_{NOMA} = \sum_{i=1}^{N_U} \sqrt{p_t \, \alpha_i} \, x_i, \qquad\qquad (3.1)$$

where N_U is denoted to represent the number of users. However, here, for two users, it has been assumed near and far users are identified with N and F symbols, respectively.

The received signals at the two relays are defined as Y_f and Y_n and can be written as:

$$Y_i = H_i \, x_{NOMA} + w_i, \qquad i \in \{F, N\} \qquad\qquad (3.2)$$

in which H_F and H_N are the channels for far and near relays, respectively, with $\left\|H_F\right\|_F^2 < \left\|H_N\right\|_F^2$, where $\left\|A\right\|_F$ represents the Frobenius

normalization of the matrix A. It is noteworthy that $\left\|H\right\|_F^2 = trace(H \times H^H)$ is exploited to measure the channel gain. In more detail, this process is obtained as:

$$\left\|H\right\|_F^2 = trace(H \times H^H),$$

$$= \sum_{n=1}^{N_{rx}} \sum_{m=1}^{N_{tx}} |H(n,m)|^2 = \sum_{k=1}^{n} |\lambda_k|^2, \qquad (3.3)$$

in which λ_k are the eigenvalues associated with the eigenvectors of the MIMO channel matrix. An alternative method is employed as detailed in [66][67][68] by using generalized singular value decomposition (GSVD), which is considered as an efficient technique for channel evaluation. It is noteworthy that the two methods can be applied to any number of transmitting and receiving antennas, i.e., squared and non-squared channels.

Furthermore, $w_F \sim CN(0, \sigma_{w_F}^2)$ and $w_N \sim CN(0, \sigma_{w_N}^2)$ are the additive white Gaussian noise (AWGN) at the far and near relay terminals, with zero mean and variance of $\sigma_{w_F}^2$ and $\sigma_{w_N}^2$, respectively. The DF relays achieve processing for the received NOMA signals, whereas the far relay implements direct detection for the incoming signal without the need to apply SIC. This detection starts with equalizing the channel by using ZF equalization, then detecting the transmitted symbols, x_F. These symbols are transmitted to the first user, U_1, via mmWave channel.

For the near relay, the SIC process is compulsory for signal construction from the entire incoming NOMA signal as explained in algorithm 3.2. After applying SIC, the detected symbols of the near relay are forwarded to the second user, U_2.

At the far relay, the throughput can be evaluated as:

$$R_F = \log_2(1 + \gamma_F), \quad\quad\quad (3.4)$$

where γ_F is the SINR at the far relay and is expressed as:

$$\gamma_F = \frac{p_t \alpha_F \|H_F\|_F^2}{p_t \alpha_N \|H_F\|_F^2 + \sigma_{w_F}^2}, \quad\quad\quad (3.5)$$

On the other hand, the throughput at the near relay terminal is calculated as:

$$R_n = \log_2(1 + \Omega_N), \quad\quad\quad (3.6)$$

where Ω_N is the SNR at the near relay after applying SIC, after removing the far relay's signal. The SNR (Ω_N) is:

$$\Omega_N = \frac{p_t \alpha_n \|H_N\|_F^2}{\sigma_{w_N}^2} \quad\quad\quad (3.7)$$

3.2.2 Second Hop from Relay to User (Access Link)

Transmission over mmWave is another promising technology that has recently gained significant attention in the wireless communication community due to its potential to provide high data rates and large bandwidth. There are several types of large-scale path losses analyzed in this study, as shown in Table 3.1.

Table 3.1: Path loss exponent (PLE) for different environments scenario[69].

Environment Scenario	PLE
Free-space	2
Urban-area	(2.7-3.5)
Suburban-area	(3-5)
Line of sight for indoor	(1.6-1.8)

Algorithm 3.1: Paring Algorithm for NOMA Relays with PAF Evaluation [16]

Input← all BS-Relays channels gains, $\{H_1, H_2, \ldots, H_{2K}\}$, number of groups, (K), number of relays, $(2K)$, and number of users, $(2K)$.

Input← The target rates for all users that are connected to the relays, $\{r_1, r_2, \ldots, r_{2K}\}$

1. The gains of BS-relays channels are sorted in descending order, i.e. $\left\|H_1\right\|_F^2 \geq \left\|H_2\right\|_F^2 \geq \cdots \geq \left\|H_{2K}\right\|_F^2$ in which the first half contains the channels of relays with higher channel gain, and the 2nd half would be for relays the lower channel gain, i.e. $\{\left\|H_1\right\|_F^2, \left\|H_2\right\|_F^2, \ldots, \left\|H_K\right\|_F^2, \left\|H_{K+1}\right\|_F^2, \ldots, \left\|H_{2K}\right\|_F^2\}$.

2. Do pairing of the 1st relay in the first half, i.e. relay with channel H_1, with the 1st relays of the 2nd half, relay with channel H_{k+1}.

3. Removing the paired relays from the list, and repeat 2, until all relays are paired into K groups.

4. According to the given target rates of all users, evaluating the PAFs for the paired relays, by giving the user with a lower channel gain a higher PAF, while the other user would have the rest of the power.

5. Do 4 for all pairs.

6. Examining the achieved rates for all users, and calculate the gap between the obtained and the required rate.

7. If the gap is less than a threshold level, modify the PAF inside the pair itself, else substitute this user with a user in another pair that has a gap with a positive value, i.e., perform rate greater than its required rate.

Output: Set of pairs with the optimum PAF for each user.

It has employed CI free-space reference distance (d_o) for the path loss (PL) model of 28 GHz and 73 GHz bands. The equation for the CI model is given by [70] as:

$$PL[dB] = FSPL(d_0) + 10nlog_{10}(\frac{d}{d_0}) + X_\sigma, \qquad (3.8)$$

where n is the path loss exponent, which has measured values for LOS and NLOS. Hence, it differs from frequency to frequency in the mmWave bands. Also, the shadow factor is denoted as X_σ, which is represented by a Gaussian distribution random variable with a zero-mean and standard deviation of σ in dB. The distance between the transmitter and receiver is denoted by d in Eq. (3.8). All these factors are illustrated in Table 3.2 for the frequencies utilized in this study, and for measurements achieved by [70],[49] over antennas at the transmitter and receiver with isotropic gains defined in dB_i as G_{tx} and G_{Rx}, respectively.

Table 3.2: summarizes the PLE (n) and standard deviations (σ) of the shadowing factor ($X\sigma$) for the frequencies 28 GHz and 73GHz at d_0= 1m [70][49].

Frequency (GHz)	G_{TX}/G_{RX} [dBi]	LOS		NLOS	
		n	$X\sigma$[dB]	n	$X\sigma$[dB]
28GHz	24.5/24.5	1.9	1.1	4.5	10.0
73GHz	27/27	2.4	6.3	4.7	12.7

DF relays decode the signals after they have been received from the source and send the decoded signals to the destinations after changing the carrier to mmWave frequencies. To prevent error propagation, the relay

successfully decoded estimates before sending them to the destination [71].

After extracting the signal of the intended user from the incoming NOMA signal at the far and near relays, the relays forward the decoded signals to U_1 and U_2. At each user terminal, the received signal can be expressed as:

$$y_{U_k} = \boldsymbol{H}_{U_k} X_k + w_{U_k} \quad k \in \{1,2\}, \tag{3.9}$$

where $w_{U_k} \sim CN(0, \sigma^2_{w_{U_k}})$ for $i \in \{1,2\}$, is denoted for the AWGN at each user terminal.

As the access hops are achieved via conventional orthogonal multiple access OMA, the capacity of this link for the two users can be evaluated as:

$$R_{U_k} = \frac{1}{2} \log_2(1 + \frac{p_t \|H_k\|_F^2}{\sigma^2_{w_{U_k}}}) \quad k \in \{1,2\}, \tag{3.10}$$

in which half refers to the use twice of the bandwidth for the OMA access link, while for the NOMA system in the backhaul link, this factor was equal to one, since half of the bandwidth is exploited compared to OMA.

The end-to-end (E2E) rates for the two links at the two users' terminals are easily calculated as:

$$R_{T_1} = \min(R_F, R_{U_1}),$$

$$R_{T_2} = \min(R_N, R_{U_2}), \tag{3.11}$$

in which the lower capacity for any link would be dominant for that link. Furthermore, the achievable sum rate, R_T, which achieved by the BS can be evaluated as:

$$R_T = E\{R_{T_1} + R_{T_2}\}, \tag{3.12}$$

where $E\{.\}$ is denoted for the expectation process, which represents the mean of the achievable throughput of the two users.

Algorithm 3.2: SIC at the near user terminal

Input: H_N and Y_N

1. Apply ZF equalization to remove the effect of the channel, H_N. i.e.,
   $$\overline{x}_{NOMA} = \frac{Y_N}{H_N} = x_{NOMA} + \frac{w_N}{H_N}$$
2. From $\overline{x}_{NOMA}$, x_F is detected directly since it has higher superposed power.
3. Convolve the detected x_F with H_N, to create the far user signal over the near user channel, i.e., $H_N x_F$.
4. $H_N x_F$ is subtracted from the entire received NOMA signal, i.e., $Y_N - H_N x_F$, for construction of the near relay's signal with a level of inherent noise, i.e. $H_N x_N + w_N$.
5. Apply equalization to the signal obtained in 4, i.e. $\overline{x}_N = x_N + \frac{w_N}{H_N}$.
6. The noisy version of the near symbol user, $\overline{x}_N$, is then obtained and converted to bits depending on the modulation scheme used already at the BS.

Output: The interference-free near-user signal $\overline{x}_N$.

3.3 Complexity Analysis of The Proposed System

In this section, the arithmetic complexity of the proposed MIMO-NOMA is presented, in which the number of arithmetic operations such as matrices multiplication, the inverse of a matrix, and addition, that are required to complete the processing of the received signal at each node, are evaluated. As mentioned earlier that each receiving terminal, i.e., at the DF relay and the user receiver, is required to apply a ZF equalizer to remove the effect of the channels. Moreover, it is required to apply SIC at all nodes operating with

NOMA except the higher order node, which is the furthest node from the service provider or the node that allocated a higher portion of the available power. Thus, in this section, it has been evaluated the number of operations required to accomplish the reception of the signal. Following the athematic complexity derived in [72], can be obtained the computational operations required to perform ZF and SIC at each relay. All nodes are equipped with N_{tx} transmitting antennas, N_{rx} receiving antennas, and for K DF relays, each one is connected to a user. According to this system's parameters, the required number of matrix inversion is K, while the number of SIC operations is K-1. Furthermore, the mathematical complexity can be expressed as $\mathcal{O}(KN_{tx}N_{rx}^3)$.

3.4 Simulation Results

In this section, two hops for the signals from a BS to two users are assumed, i.e., backhaul and access links. Multiple cases are considered to evaluate the error probability, system capacity, and outage probability. Rayleigh fading channels are assumed for the sub-6 GHz backhaul link, i.e., the link from the BS to the relays, while mmWave frequency is considered in the access link between the relays and users. All details about the two links are defined in Table 3.3.

In the first hop, the relay associated with the U_1 is assumed to be far from the BS. It has been assumed the distance between them as $d_1 = 500m$, and the PAF is $\alpha_1 = 0.7$. On the other hand, the relay associated with U_2 is assumed in a near position to the BS, in which the distance is denoted and assumed as d_2 = $300m$, with a PAF of $\alpha_2 = 0.3$. On the other hand, the access link between the DF relays and the users exploits the mmWave band with 28GHz or 73GHz. In this link, it has been assumed without the loss of generality that the two users have the same distance from their corresponding relays, i.e., $d_3 = d_4 = $

$100m$, OMA is used in this link. It is noteworthy that the modulation scheme exploited in this study is QPSK.

Table 3.3: Simulation parameters and notations.

Notation	Parameter	Value
(f_a, BW)	(Operating frequency for the access link, Bandwidth)	(28GHz, 100MHz) and (73GHz, 2000MHz)
(f_b, BW)	(Operating frequency for the backhaul link, Bandwidth)	(3.5GHz, 25MHz) [73]
P_t	Transmitted power	[0-50] (dBm)
No	Noise power	-174dBm/Hz +10log10(BW)
α_1, α_2 $\in \{0,1\}$	PAFs for the near and far relays, respectively.	$\alpha_1 + \alpha_2 = 1$
Modulation Scheme	QPSK	$\frac{1}{\sqrt{2}}(\pm 1 \pm j1)$

3.4.1 Backhaul link and mmWave access link of 28GHz

In this scenario, a sub-6 GHz band of 3.5GHz with 25MHz bandwidth is assumed to work with MIMO-NOMA in the backhaul link, i.e. the link between the BS and the relays. The access link, between the relays and the user, exploits mmWave mode of 28GHz with 100MHz bandwidth to transmit the detected data by the DF relays to the users over different transmitted

powers in (dBm). Figure 3.2 shows the throughput obtained by each user with the achievable sum rate applied by the BS. It has been considered in this simulation that $N_{tx} = N_{rx} = 2$ for all terminals of the two hops. Moreover, the distances between the nodes are mentioned in the caption of this figure as defined earlier in this section.
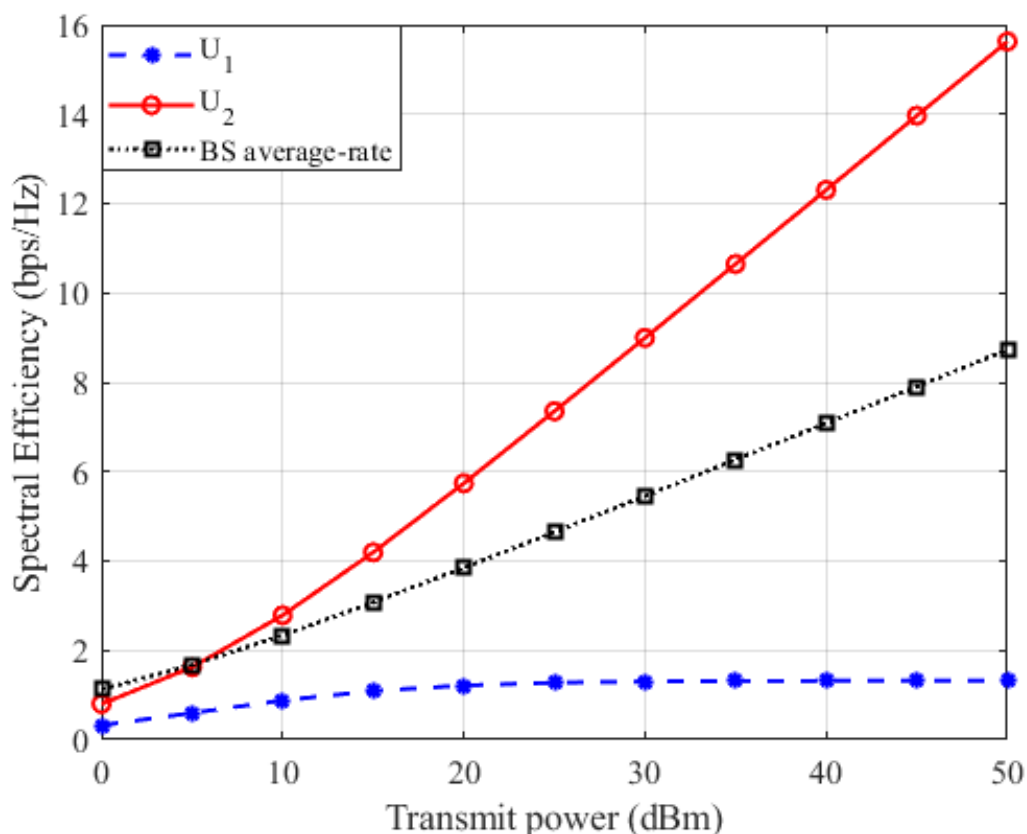
Figure 3.2: E2E spectral efficiency of two users with $d_1 = 500m$, $d_2 = 300m$, and $d_3 = d_4 = 100\ m$, $N_{tx} = N_{rx} = 2$.

It is observed that the near user achieves better spectral efficiency than the far user because of employing SIC to remove the signal of the far user as discussed earlier in this study. Moreover, the far user's spectral efficiency becomes saturated after approximately 25 dBm, with 1.68 bps/Hz. The average rate achievable capacity is calculated by taking the mean of the sum of the spectral efficiency of the two users.

Figure 3.3 shows the outage probability of this scenario. The outage probability is the probability that the rate in bits/sec/Hz (bps/Hz) goes below the minimum threshold level required for a user. It can be seen that U_1, which is connected to the far relay, with a higher PAF of 0.7, has an outage probability of about 1dBm better than the outage probability of U_2, which is connected to the near relay, with a lower PAF of 0.3, when the target rates for the U_1 and U_2 are considered as $r_1 = 1$ bps/Hz and $r_2 = 3$ bps/Hz, respectively. Furthermore, it can be noticed that increasing the number of antennas at the BS for both links reduces the transmitted power by more than 5dBm. A significant role is played by the PAF in optimizing the performance of the two users and the entire system. This can be achieved by verifying this factor depending on the required rate of each node.
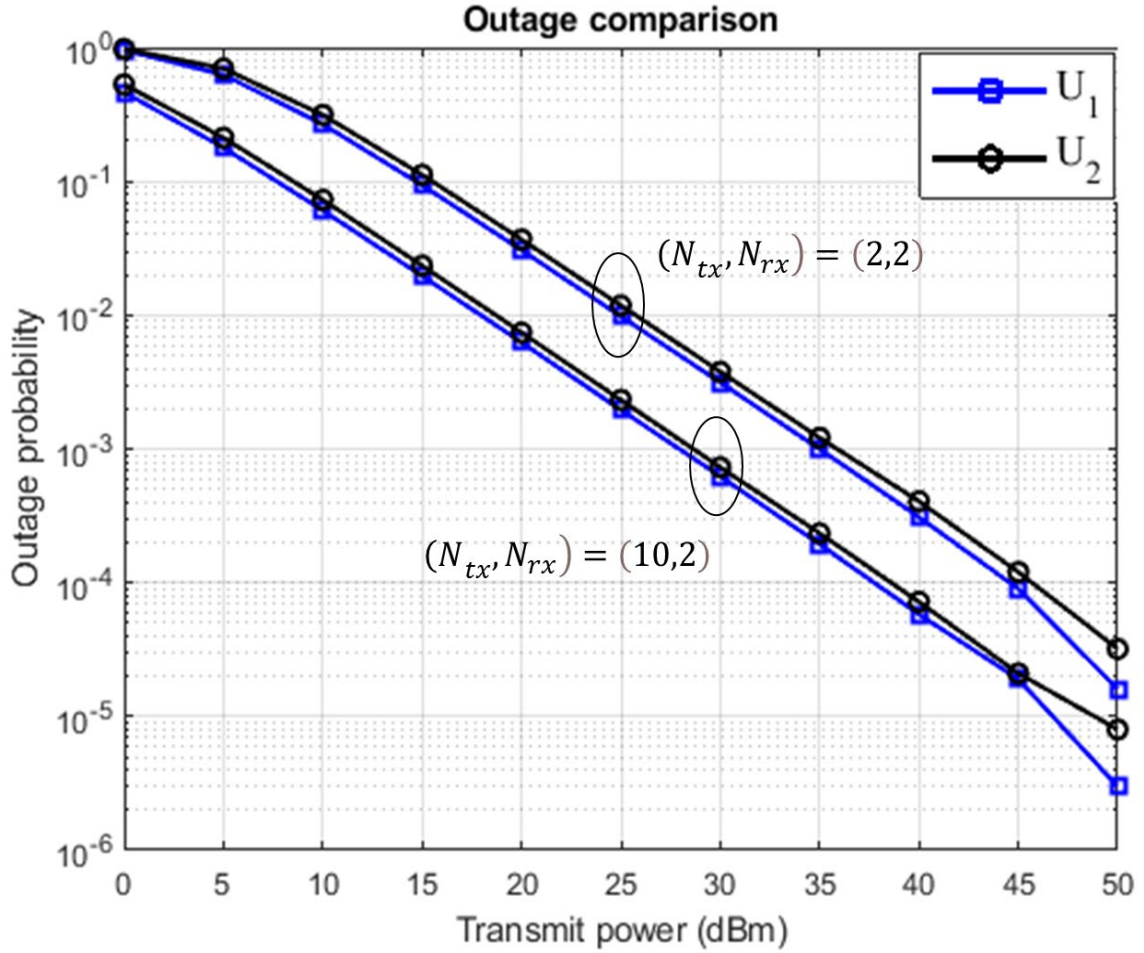
Figure 3.3: The outage probability of two users with $d_1 = 500m$, $d_2 = 300m$, and $d_3 = d_4 = 100\,m$, $(N_{tx}, N_{rx}) = (2,2)$ and $(10,2)$, the target rates are assumed $r_1 = 1$ and $r_2 = 3$ bps/Hz.

In this scenario, the BER over different transmitted powers in (dBm) is shown in Fig.3.4. In this figure, two scenarios have been taken into account by changing the number of antennas in the BS from 2 to 4, while keeping the number of antennas in receiver terminal of the relay, and the user with two antennas. It can be noticed from this figure that an increase in the transmitting antennas gives more than 25 dBm improvement in this performance metric at 10^{-4} BER.
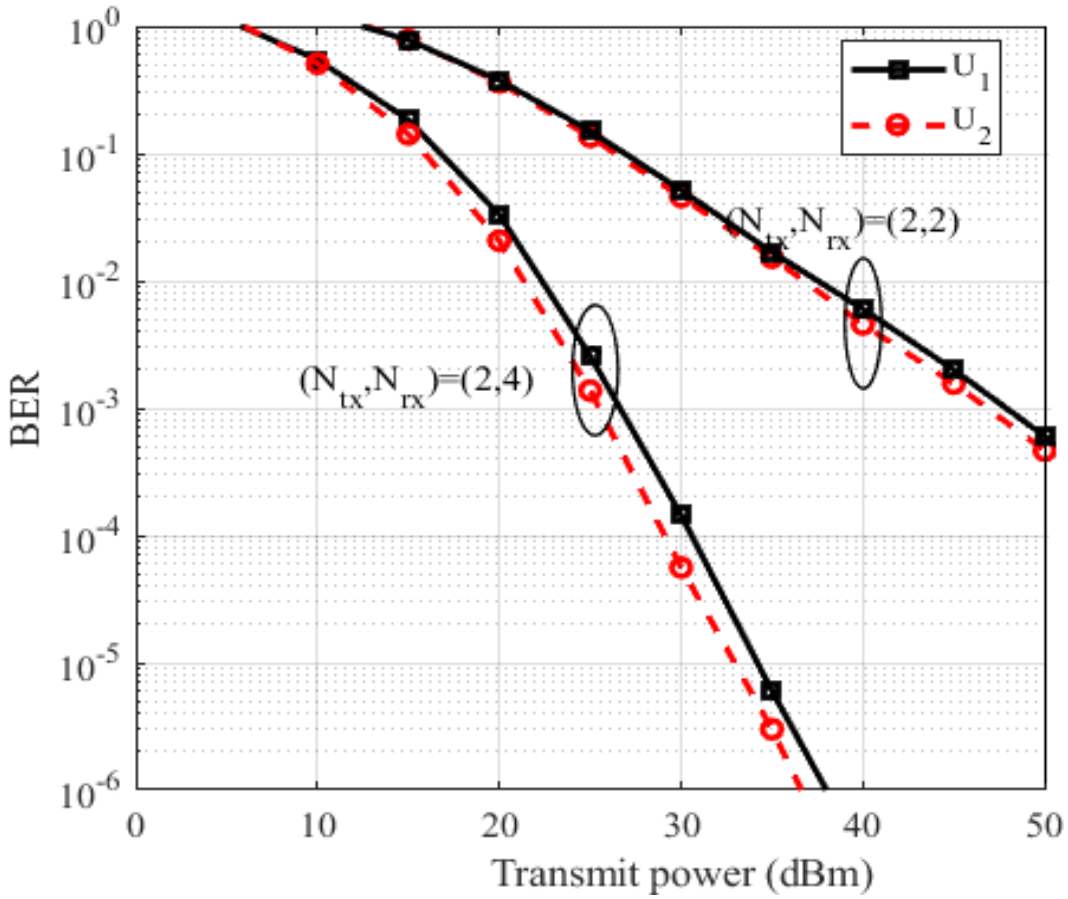
Figure 3.4: E2E BER of two users over 28GHz access link, with $d_1 = 500m$, $d_2 = 300m$ and $d_3 = d_4 = 100\ m$, $(N_{tx}, N_{rx}) = $ (2,2) and (2,4).

Moreover, by utilizing 28 GHz in the access link, Fig.3.5 shows a three-dimension (3D) plot for the E2E spectral efficiency of the proposed system over a different number of transmitting antennas, N_{tx}, and with a range of transmitted power, Pt in dBm. It can be seen that increasing the number of antennas in the BS of the proposed system can significantly improve the spectral efficiency and this increase in N_{tx} can satisfy spectral efficiency with a minimum required Pt with $N_{rx}=2$. Furthermore, this plot indicates the required power at a specific N_{rx} to achieve an intended spectral efficiency.
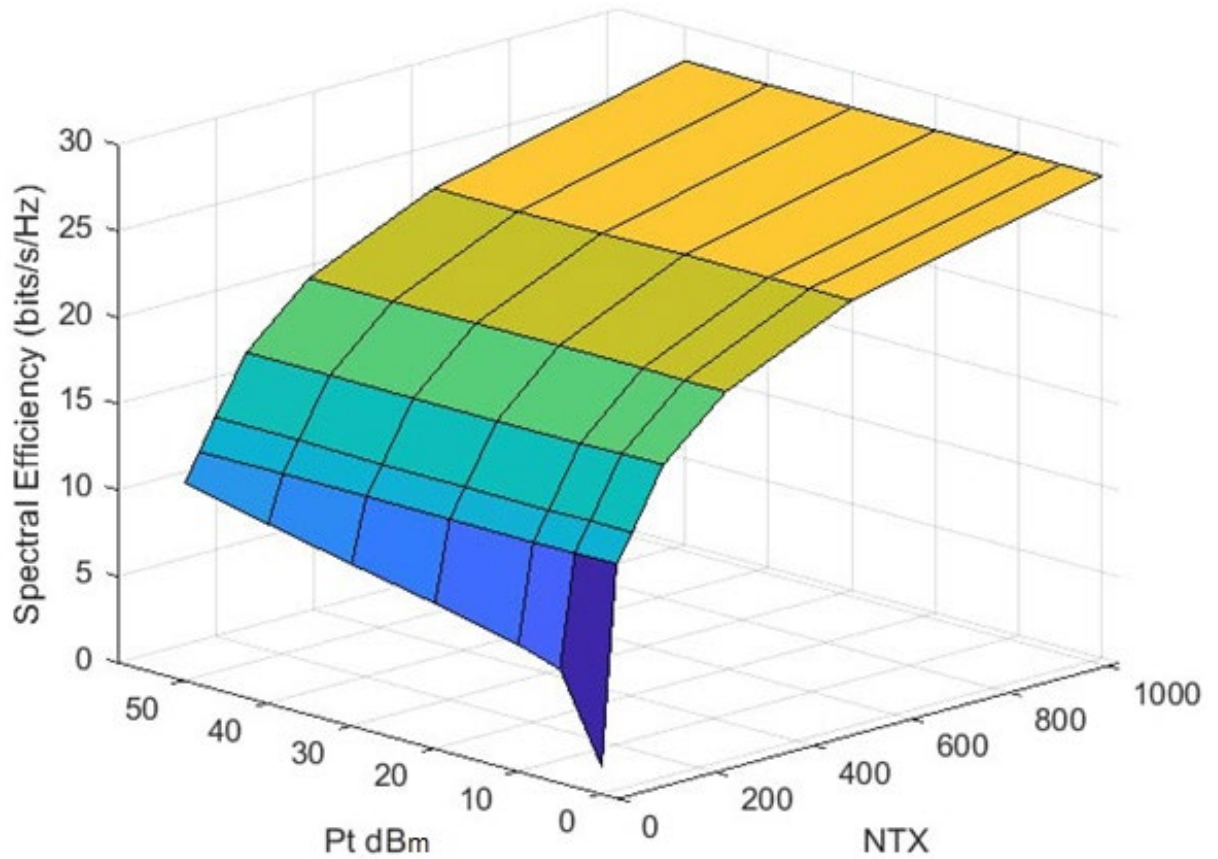
Figure 3.5: 3D-E2E spectral efficiency for different numbers of transmitted antennas at each terminal, N_{tx}, and several values of transmitted power Pt (dBm) with $N_{rx}=2$.

3.4.2 Compassion for access links with 28GHz and 73GHz

In the second part of the simulation results, it has been introduced a compassion between two mmWave frequency bands, which are 28GHz and 73GHz. This compassion can be achieved by changing the band of the access link of the proposed system between these two bands. Three performance metrics have been considered to implement this compassion, which is the spectral efficiency of the BS, the outage probability, and the error probability, which is represented by the BER. In Fig.3.6, the sum rate produced by the BS

is obtained for the two mmWave bands, in which the spectral efficiency of the two users is evaluated in the two hops and taking the minimum Ergodic capacity for each link, i.e. the minimum capacity at any link would be dominant, then by evaluating the mean of the summation of the two users capacity, the spectral efficiency of the BS is obtained. It can be seen that the 28GHz mmWave band outperforms 73 GHz over all transmitting power ranges, with more than 7bps/Hz at Pt=50dBm. In this figure simple MIMO case of $(N_{tx}, N_{rx}) = (2,2)$ has been considered.
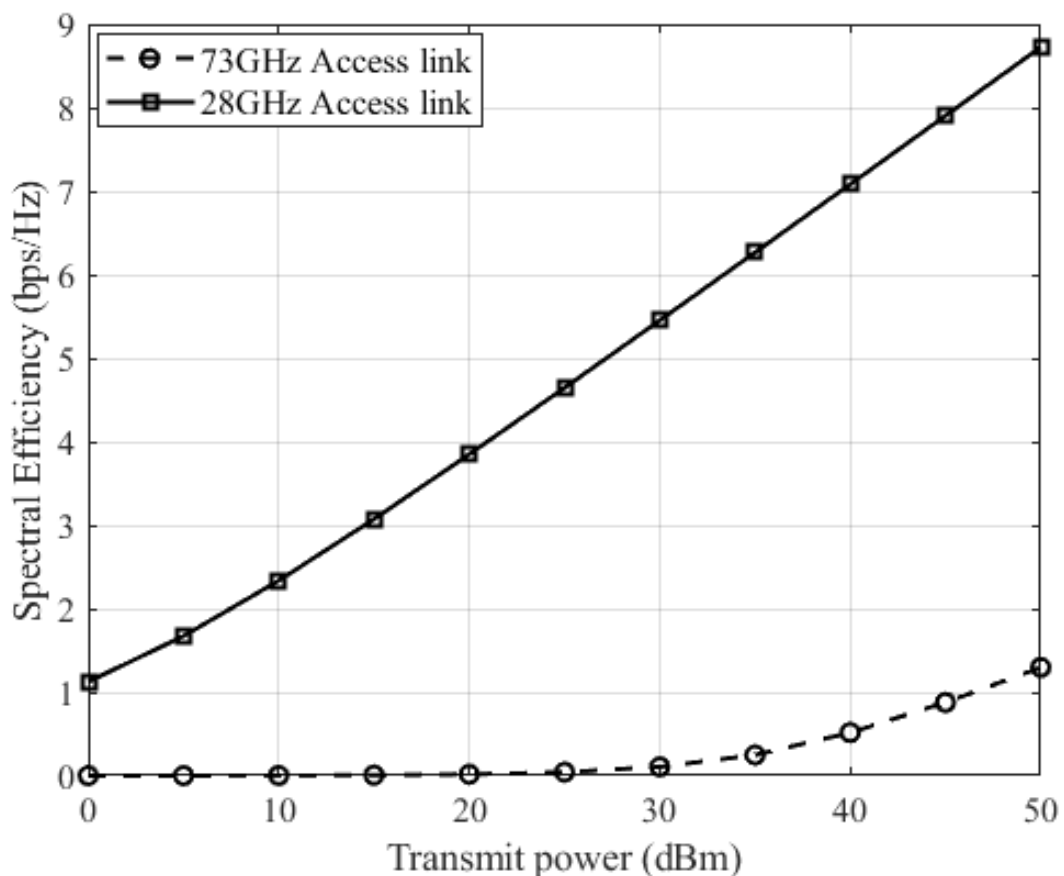
Figure 3.6: The BS spectral efficiency for the E2E system for access links of 28 and 73 GHz, $d_1 = 500m$, $d_2 = 300m$ and $d_3 = d_4 = 100\ m$, $(N_{tx}, N_{rx}) = (2,2)$.

Figure 3.8 shows the E2E BER for those mmWave frequency bands which are operating in the access link of the two users. In this simulation, it

has been increased the number of antennas at each receiving terminal to 10, while keeping the transmitting antennas at 2 as before. Again, it can be seen that the band of 73GHz needs about 15dBm transmitting power from the BS to satisfy the same BER at 10^{-5}. The purpose of this figure is to comapre two mmwave frequencies which are 28GHz and 73GHz over a NOMA system that serves two users.
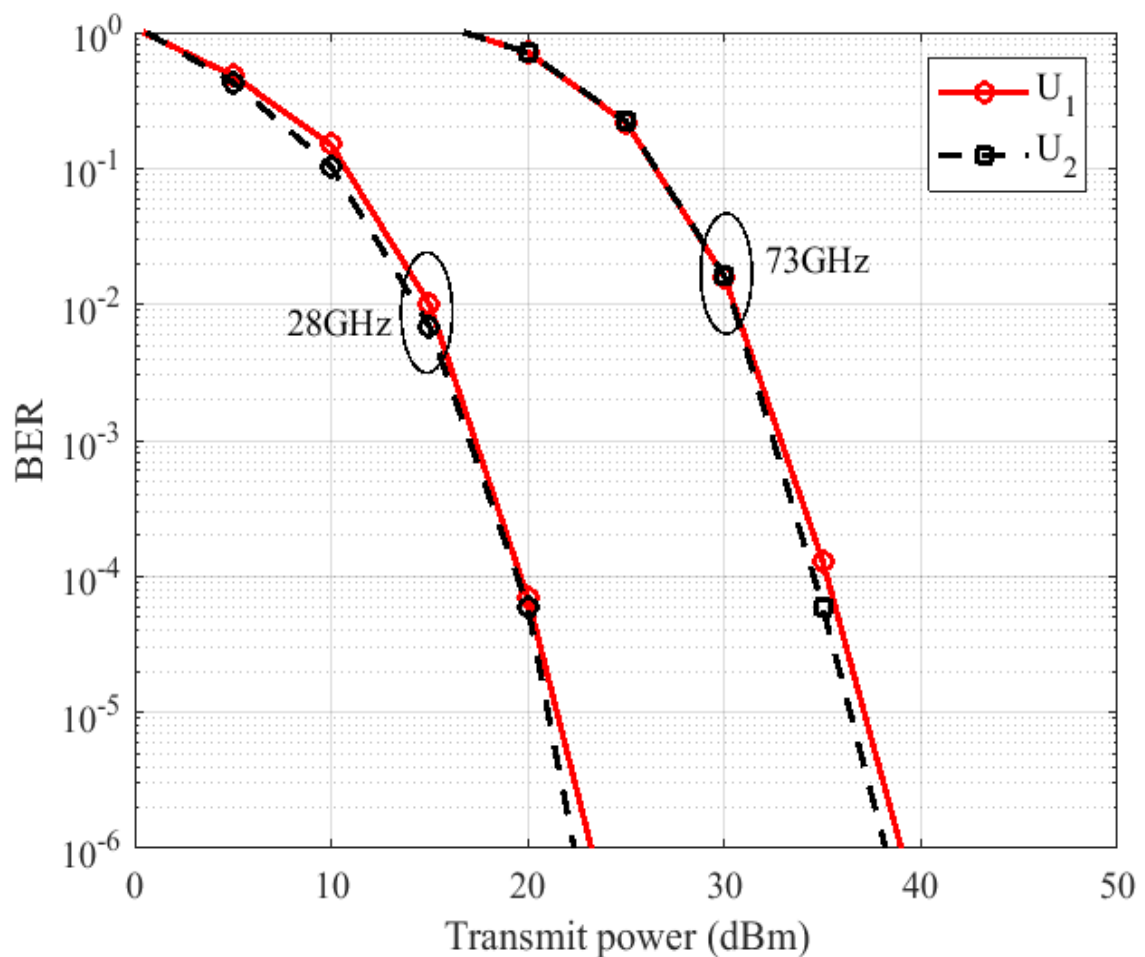
Figure 3.8: BER comparison of two users with $d_1 = 500m$, $d_2 = 300m$ and $d_3 = d_4 = 100\ m$, $(N_{tx}, N_{rx}) = (2,10)$, $\alpha_1 = 0.7$, $\alpha_2 = 0.3$.

CHAPTER FOUR

MULTIUSER BEAMFORMING SYSTEM WITH MASSIVE MIMO-NOMA OVER MMWAVE CHANNEL

4.1 Introduction

In this chapter, massive MIMO with NOMA is considered to serve multiple users wirelessly over mmWave channels. A BS with tens of antennas is proposed to provide services to users in the coverage area by applying ZF and MRT beamforming techniques. The BS first divides the area into clusters that contain only two users via applying a pairing algorithm, then NOMA is applied to the two users by providing different power allocation factors for satisfying user fairness, and depending on users' circumstances. The achievable throughput for each user in the cluster along with the sum-rate provided by the BS are analyzed and evaluated for the two beamforming mechanisms. The results are obtained for different numbers of BS antennas over different combinations of power allocation coefficients. The simulation results reveal the improvement obtained by increasing the antennas in the BS. Additionally, the two beamforming methods introduce similar throughput when the same parameters are considered, with slight outperforming of MRT in the outage portability.

4.2 System Modeling

In this chapter, one BS with N_{Tx} number of antennas, K potential users, each of which has N_{Rx} antennas have been considered. The system under consideration is assumed to work in the downlink mode as shown in Fig.4.1. For more clarification, the k_{th} user is denoted as U_k. To offer multiuser downlink transmission, the BS simultaneously transmits K beams, each beam supports a cluster with two users or more for serving the users in a particular

cluster via the NOMA technique. In this chapter, it is assumed that each cluster has two users only. This assumption can be achieved in practice by utilizing a pairing algorithm for the sake of reducing the complex process in the BS. Furthermore, to obtain the full benefits of NOMA, the BS examines the channel gain for each user in a particular cluster. For two users in a cluster, U_1 is denoted for the user who has weak channel gain, i.e. the far user or the user that suffers from high attenuation circumstance. Whereas U_2 is denoted for the second user in that cluster with the higher channel gain. The channel gains for those users are denoted as $\boldsymbol{H}_1 \in \mathbb{C}^{N_r \times M}$, $\boldsymbol{H}_2 \in \mathbb{C}^{N_r \times M}$, respectively. At the BS, beamforming is applied for each user as $\boldsymbol{s}_{U_k} = \sum_{i=1}^{N_r} \boldsymbol{w}_{i,k} \, x_k$, with power p_t, here $\boldsymbol{w}_{i,k} \in \mathbb{C}^{M \times N_r}$ is the beamforming weight for the k_{th} user, it is worth noting that p_t represents the overall transmitted power at the BS. Besides, x_k represents the k_{th} user's symbols after applying the modulation scheme. The superposed transmitted NOMA symbol for the users in a particular cluster is expressed as $\boldsymbol{x}_{NOMA} = \sqrt{\alpha_1} \, \boldsymbol{s}_{U1} + \sqrt{\alpha_2} \, \boldsymbol{s}_{U2}$, where $\boldsymbol{s}_{U1}$ and $\boldsymbol{s}_{U2}$ are the transmitted symbol for U_1 and U_2 users, respectively. Besides, $\alpha_k \in (0, 1]$ is the k_{th} user power allocation coefficients. The BS allocates α_k for the k_{th} user in a particular cluster depending on its knowledge of the CSI of that user, in which the user with a weak channel is given more portion of p_t than the user with strong channel conditions. It is noteworthy that the BS is assumed to have full knowledge of the CSI of all users, as the channel estimation is out of the scope of this thesis.
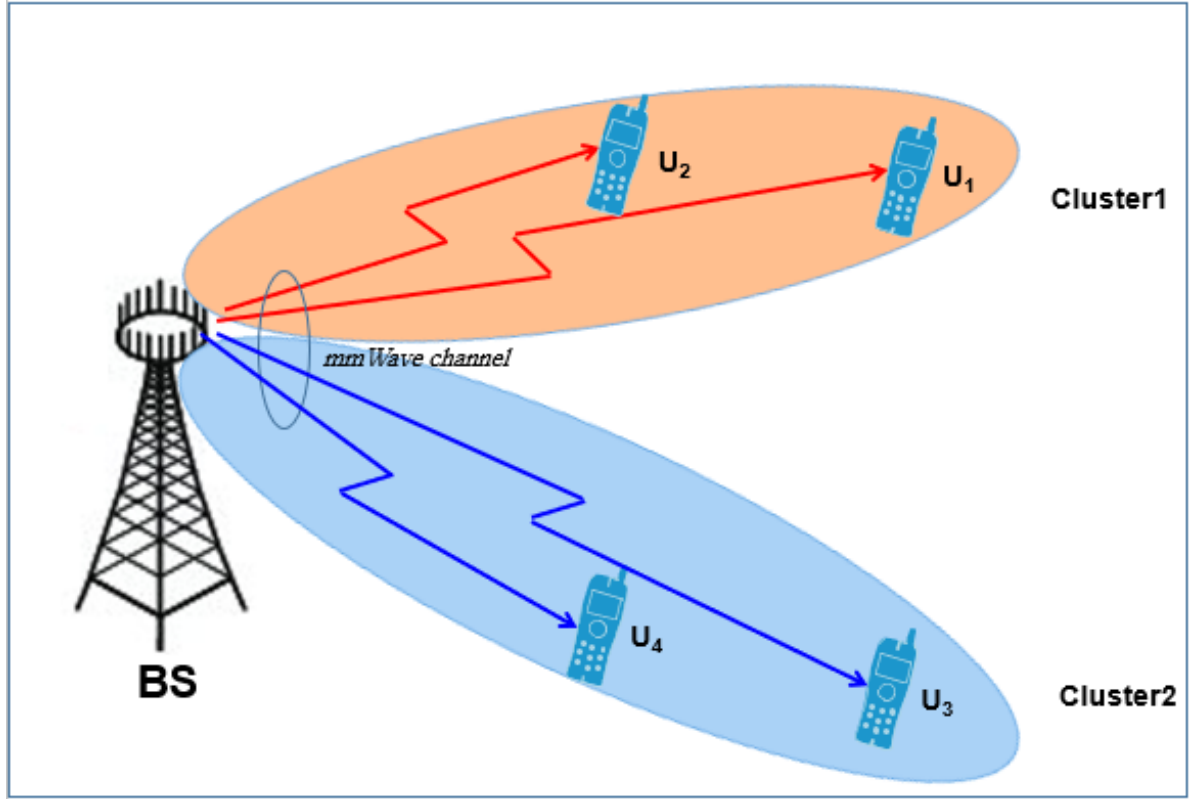
Figure 4.1: Two clusters of NOMA with beamforming to serve two users in each cluster over the mmWave channel.

The received signal for the k_{th} user, $\boldsymbol{y}_k$, can be written in different expressions depending on the definitions explained earlier as:

$$\boldsymbol{y}_k = \sqrt{p_t}\,\boldsymbol{H}_k \boldsymbol{x}_{NOMA} + \boldsymbol{n}_k, \tag{4.1}$$

$$\boldsymbol{y}_k = \sqrt{p_t}\,\boldsymbol{H}_k (\sqrt{\alpha_1}\,\boldsymbol{s}_{U1} + \sqrt{\alpha_2}\,\boldsymbol{s}_{U2}) + \boldsymbol{n}_k, \tag{4.2}$$

$$\boldsymbol{y}_k = \sqrt{p_t}\,\boldsymbol{H}_k \left(\sqrt{\alpha_1}\,\sum_{i=1}^{N_r} \boldsymbol{w}_{i,1}\, x_1 + \right.$$
$$\left. \sqrt{\alpha_2}\,\sum_{i=1}^{N_r} \boldsymbol{w}_{i,2}\, x_2 \right) + \boldsymbol{n}_k, \tag{4.3}$$

where $\boldsymbol{n}_k \sim \mathcal{CN}\left(0, \sigma_{n_k}^2\right)$ is the AWGN with zero mean and variance equal to $\sigma_{n_k}^2$.

The last expression of (3) can be simplified more to be written as:

$$y_k = \sqrt{\alpha_1 p_t}\, H_k \sum_{i=1}^{N_r} w_{i,1}\, x_1 +$$

$$\sqrt{\alpha_2 p_t}\, H_k \sum_{i=1}^{N_r} w_{i,2}\, x_2 + n_k, \qquad (4.4)$$

the first term to the right of the equality sign in (4.4) represents the signal of interest related to the k_{th} user, while the second term represents the interference caused by the second user in the cluster.

The k_{th} user's received SINR, γ_k, can thus be written as [74]:

$$\gamma_1 = \frac{\Omega_1 \|H_1 \sum_{i=1}^{N_r} w_{i,1}\|^2}{\Omega_2 \|H_1 \sum_{i=1}^{N_r} w_{i,2}\|^2 + 1}, \qquad (4.5)$$

where $\Omega_1 = \frac{\alpha_1 p_t}{\sigma_{n_1}^2}$ and $\Omega_2 = \frac{\alpha_2 p_t}{\sigma_{n_2}^2}$ represents the SNR for the first and the second users, respectively. It is noteworthy that at the first user, the interference caused by the second user is ignored as it is considered as additive noise only. This is due to allocating higher power allocation weight for this user. On the other hand, for the second user, SIC should be applied to remove the strong signal of the first user, therefore, the expression in (4.5) becomes:

$$\gamma_2 = \Omega_2 \|H_2 \sum_{i=1}^{N_r} w_{i,2}\|^2 \qquad (4.6)$$

4.2.1 ZF Beamforming

The ZF beamforming is a technique used in wireless communication to transmit signals efficiently and minimize interference between multiple antennas. The inter-user interference can be eliminated at each user using a linear precoding approach called ZF. The ZF beamforming weight for the transmitter signal from a BS to a user over a channel H is expressed as:

$$w_k = \rho H_k^H (H_k H_k^H)^{-1} \qquad (4.7)$$

with

$$\rho = \frac{1}{\sqrt{Tr(\boldsymbol{HH}^H)^{-1})}} \qquad (4.8)$$

where ρ is used for normalization purposes to avoid transmission with greater than the maximum available power at the BS. Moreover, $\boldsymbol{A}^H$, $Tr(\boldsymbol{A})$, and $(\boldsymbol{A})^{-1}$ are denoted for the Hermitian transport, Trace, and Inverse of matrix $\boldsymbol{A}$, respectively.

4.2.2 MRT Beamforming

The MRT beamforming is another linear precoding technique used in wireless communication to transmit signals efficiently and maximizes the SNR at the receiving antenna. The MRT beamforming weight for the transmitter signal from a BS to a user over a channel $\boldsymbol{H}$ is expressed as:

$$\boldsymbol{w}_k = \rho \boldsymbol{H}_k^H \qquad (4.9)$$

4.2.3 Achievable Data Rate

The achievable data rate is one way to evaluate a system's performance. The Shannon theorem expresses a formula to calculate the data rate. According to this theorem, the transmitter can transmit data through a channel at a maximum rate. The possible data rate with ZF and MRT for the system under consideration is detailed in this section under this theorem, in which the total downlink power is fixed and distributed equally among all users, if equal power allocation is utilized in orthogonal multiple access systems, or the power is allocated depending on the users' circumstances like the proposed NOMA system in this study. The channel capacity, in bits per second per hertz (bps/Hz), over the AWGN channel is calculated from the Shannon theorem by:

$$R = B\log_2(1 + \Omega), \qquad (4.10)$$

where B and Ω are the bandwidth and the SNR, respectively. For multi-user communications that apply the NOMA technique, interference plays a significant role in affecting the achievable rate. As a result, the achievable rate becomes a function of SINR instead of SNR. Hence, (4.10) can be rewritten for a k_{th} user as:

$$R_k = B\log_2(1 + \gamma_k), \qquad\qquad (4.11)$$

and the achievable sum rate for K users for any type of beamforming is given as:

$$R_{sum}^{BF} = B\ \mathbb{E}\{\textstyle\sum_{k=1}^{K} \log_2(1 + \gamma_k)\}, \qquad\qquad (4.12)$$

where $\mathbb{E}\{.\}$ is denoted for the expectation process, and beamforming $\in \{ZF, MRT\}$.

4.3 Simulation Results

In this section, it has been assumed a cluster that has two users to be served by a massive MIMO BS via applying beamforming and NOMA techniques. The two users have been chosen to be served in a particular cluster by utilizing a pairing algorithm. Inside this cluster, the two users have different channel circumstances, i.e. one of them has a channel with a strong gain, while the other has a weak channel gain. Many scenarios are considered to evaluate the system capacity and the outage probabilities over mmWave channels. All details about the simulation parameters are illustrated in Table 4.1.

Table 4.1: Simulation parameters and notations.

Notation	Parameter	Value
(f_c, BW)	(Operating frequency, Bandwidth)	(28GHz, 100MHz)
p_t	Transmitted power	[0-50] (dBm)
N_0	Noise power	-174dBm/Hz +10log10(BW)
$\alpha_1, \alpha_2 \in (0,1]$	PAFs for the near and far users, respectively.	$\alpha_1 + \alpha_2 = 1$
Digital carrier scheme	QPSK	$\pm 0.707 \pm j0.707$

Moreover, as it has been assumed mmWave channels in this study, the CI model of 28 GHz for a reference distance (d_o) is used to model this channel similar to [70] [49]as in equation 2.10.

Figure 4.2 shows the sum rate achieved by a BS that employs NOMA with ZF or MRT beamforming to serve two users. The distances of the users are assumed as $d_1 = 150m$, and $d_2 = 100m$ for U_1 and U_2, respectively. Besides, depending on the channel gains of those two users, the power allocation factors are assumed as $\alpha_1 = 0.7$ and $\alpha_2 = 0.3$. It has been assumed that the BS is equipped with a different number of antennas, i.e. $N_{Tx} = [16, 32, 64, 128]$ to work in the massive MIMO mode. Moreover, each user is assumed to have two antennas at its receiving terminal, i.e. $N_{Rx} = 2$. It can be noticed from this figure that an additional $3bps/Hz$ can be obtained when

N_{Tx} is doubled at the BS. The study has used one plot for the two beamforming techniques as it has been noticed exact results for them in this performance metric.
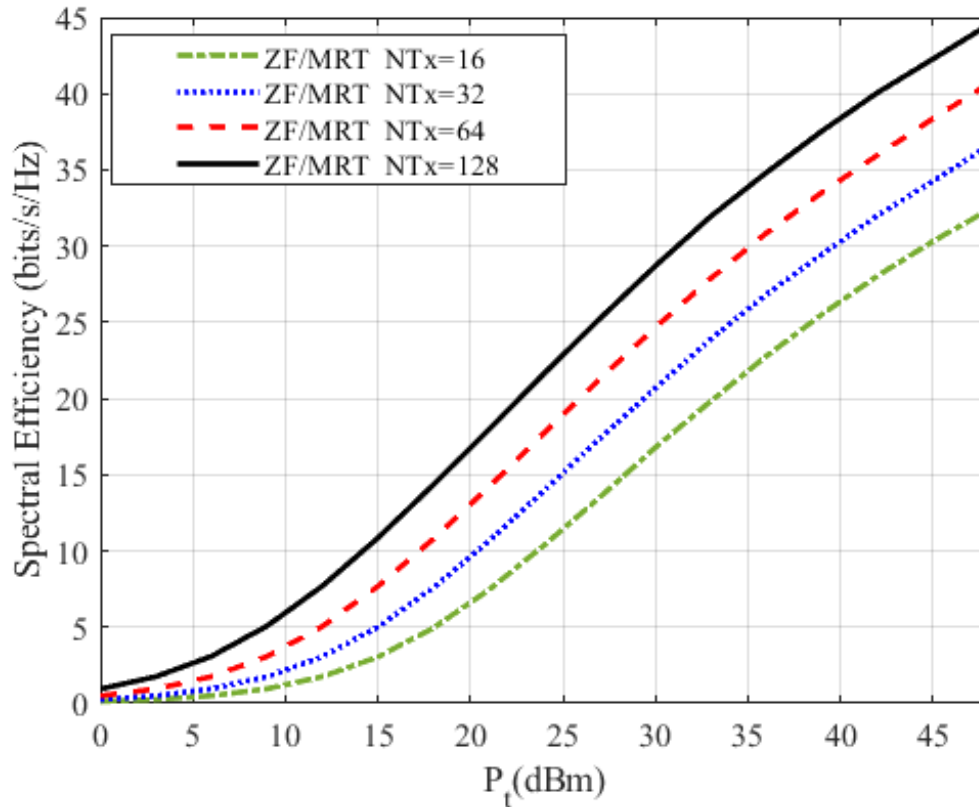
Figure 4.2: The spectral efficiency by a BS that serves two users via NOMA with ZF/MRT beamforming, $d_1 = 150m$, $d_2 = 100$, $(\alpha_1, \alpha_2) = (0.7, 0.3)$, $N_{Tx} = [16, 32, 64, 128]$, and $N_{Rx} = 2$.

In Fig.4.3, the previous setting is considered for the BS and the users. This figure shows the achievable data rate for each user over a different number of N_{Tx}. It can be seen that the near user, i.e. U_2, outperforms the far user, U_1, significantly in this performance metric. This is due to perform SIC, which is not applied at the far user depending on NOMA theory. Moreover, the far user reaches saturated rates after about $p_t = 40dBm$ due to the dominant interference at this user terminal.
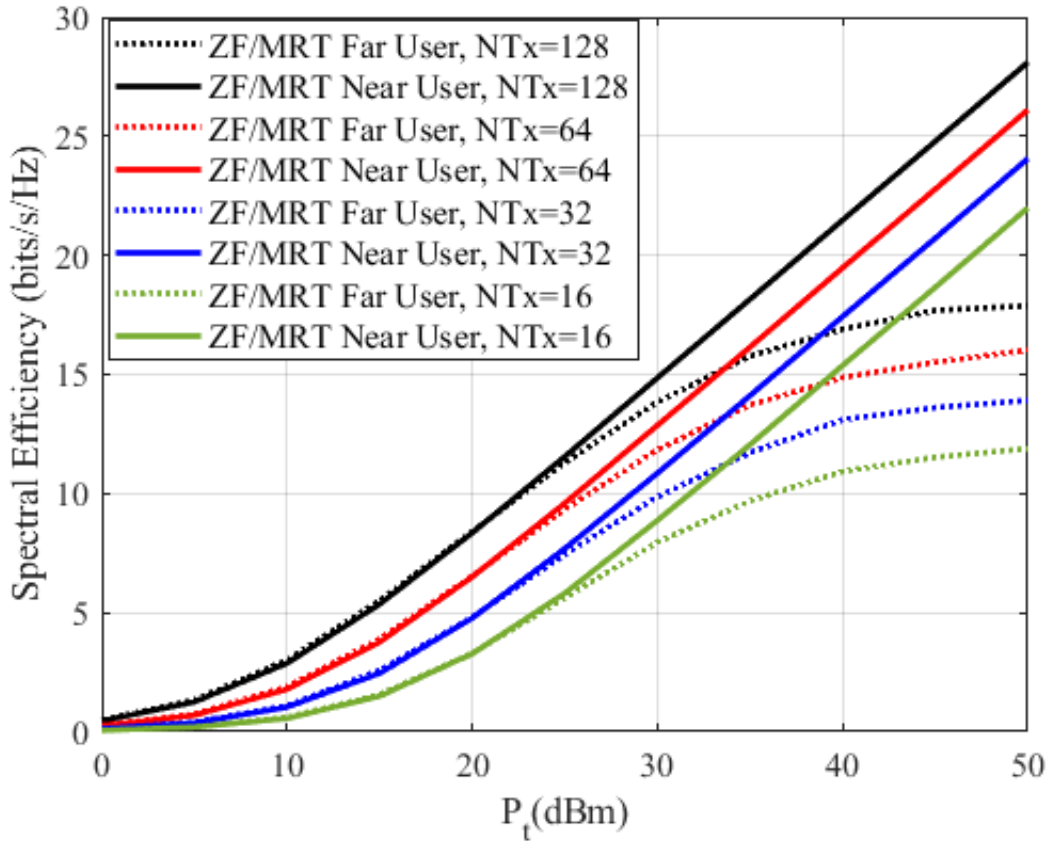
Figure 4.3: The spectral efficiency of the far and near users of NOMA with ZF/MRT beamforming, with $d_1 = 150m$, $d_2 = 100$, $(\alpha_1, \alpha_2) = (0.7, 0.3)$ $N_{Tx} = [16, 32, 64, 128]$ and $N_{Rx} = 2$.

Figure 4.4 shows the spectral efficiency for the two users, i.e. the far and the near users, which are served by a massive MIMO BS that applies NOMA with ZF/MRT beamforming. In this figure, the number of antennas at the BS is assumed 128, and the two users have two antennas. The PAF for the two users is changed using different combinations of (α_1, α_2) as $(0.7, 0.3), (0.8, 0.2)$, and $(0.9, 0.1)$. It can be seen the effect of this factor on this performance metric, that the rate of the far user is significantly increased by increasing the power allocation coefficient.
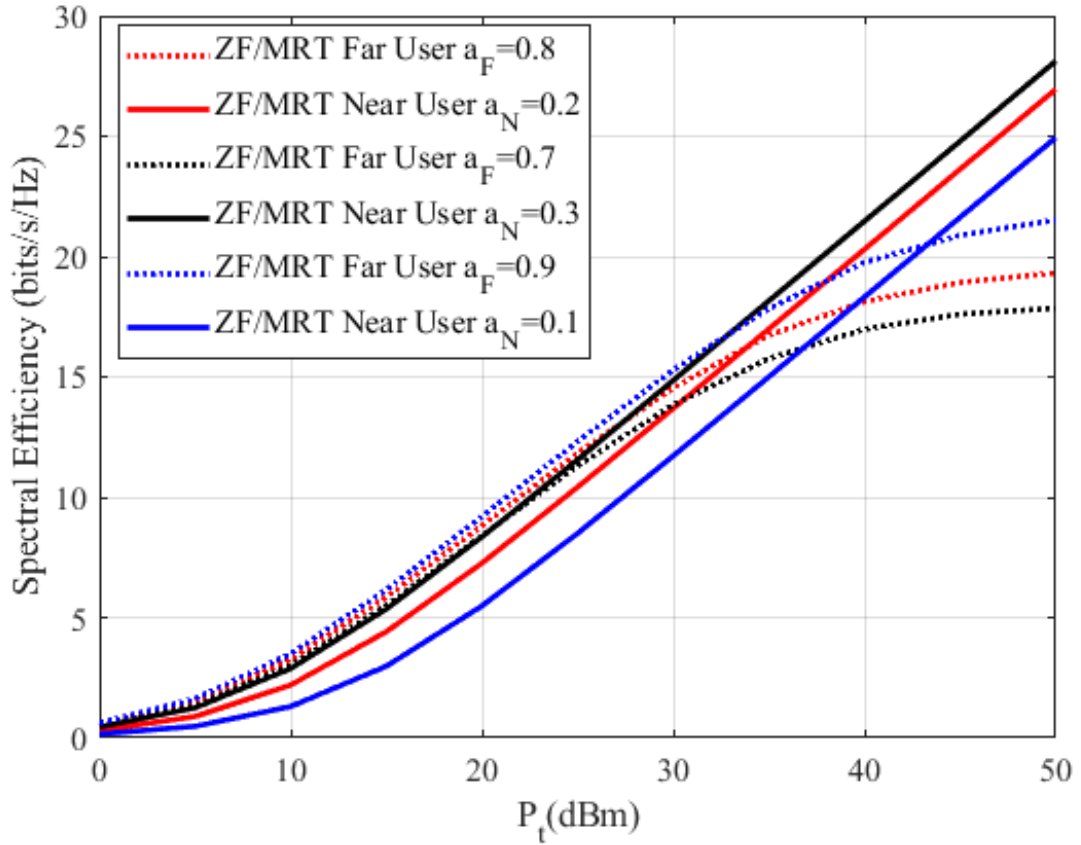
Figure 4.4: The spectral efficiency of the two users served by NOMA and ZF/MRT beamforming, with $d_1 = 150m$, $d_2 = 100$, $(N_{Tx}, N_{Rx}) = (128,2)$, $\alpha_1 = [0.7, 0.8, 0.9]$, and $\alpha_2 = [0.3, 0.2, 0.1]$.

Moreover, the outage probabilities are examined for the proposed system by employing the two beamforming techniques as shown in Fig.4.5 Two combinations of (N_{Tx}, N_{Rx}) as $(16,2)$, and $(128,2)$ are considered by assuming threshold rates for the far and the near users as $r_1 = r_2 = 7bps/Hz$. A significant improvement can be noticed in this performance metric for the two users by increasing the number of antennas at the BS to work as massive MIMO with 128 antennas. Moreover, for 16 antennas it can be seen that the MRT beamforming approach outperforms the ZF slightly.
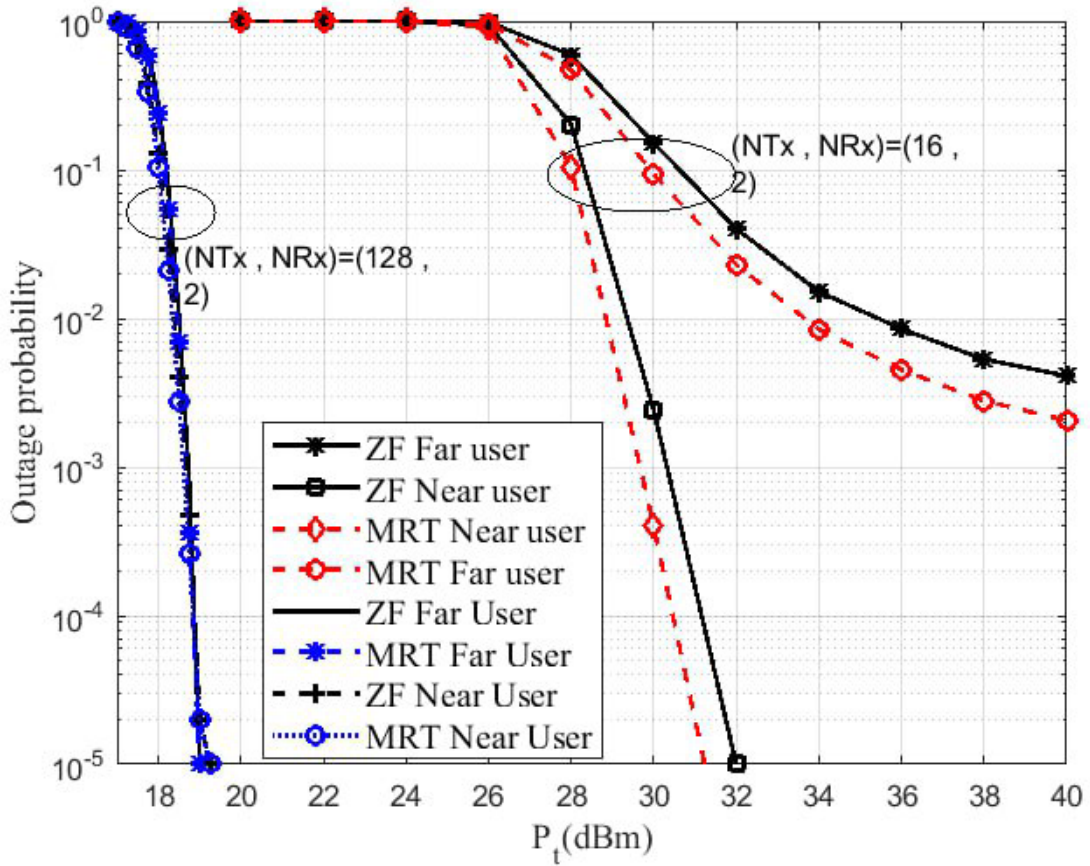
Figure 4.5: The Outage probability of the two users served by NOMA and ZF/MRT beamforming, with $d_1 = 150m$, $d_2 = 100$, $(N_{Tx}, N_{Rx}) = $ (16,2) and (128,2), with $(\alpha_1, \alpha_2) = (0.7, 0.3)$.

For more details about the case of $N_{Tx} = 128$, Fig.4.6 is drawn over more precise values of P_t to clarify the two beamforming techniques. Also, a slight improvement in outage probability can be noticed by using MRT compared to ZF.
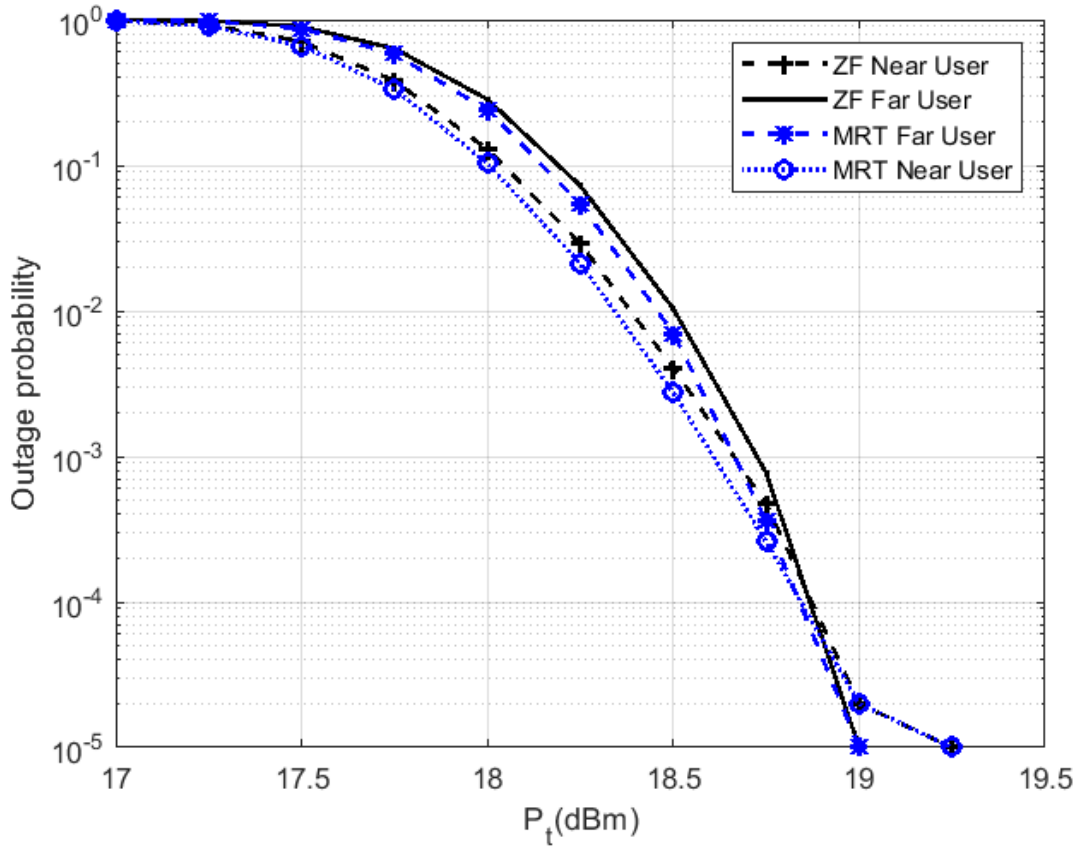
Figure 4.6: The Outage probability of the two users served by NOMA and ZF/MRT beamforming, with $d_1 = 150m$, $d_2 = 100$, $(N_{Tx}, N_{Rx}) = (128,2)$ with $(\alpha_1, \alpha_2) = (0.7, 0.3)$.

In Fig.4.7, the spectral efficiency for each user, i.e. the far and the near users, along with the BS's sum rate are shown against a different number of BS's transmit antennas, i.e. N_{Tx}. It can be noticed the effect of increasing N_{Tx} on the capacity of each user and the BS spectral efficiency. This figure is simulated with transmit power equal to $30\ dBm$, and for (α_1, α_2) equal to (0.7, 0.3).
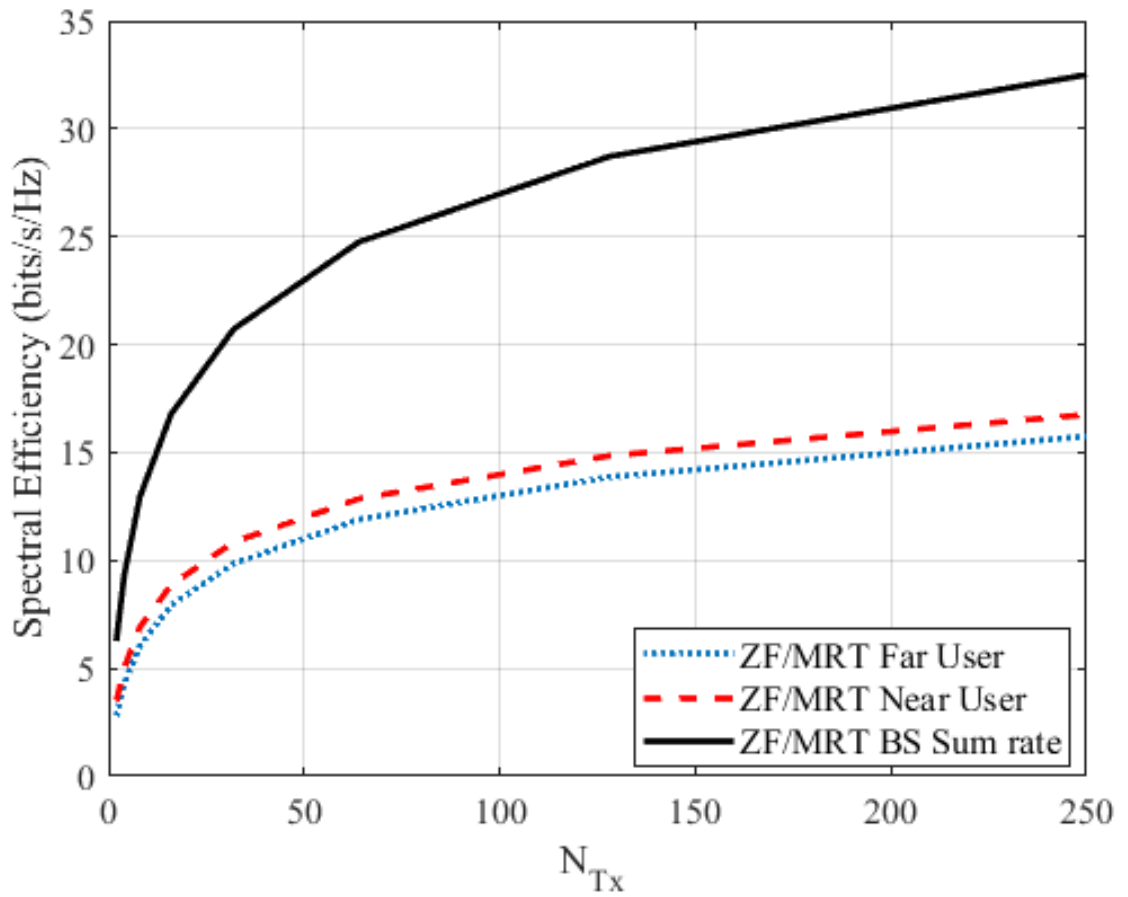
Figure 4.7: The BS's sum rate and the two users' spectral efficiency for NOMA with ZF/MRT beamforming, $d_1 = 150m$, $d_2 = 100$, $N_{Tx} = (2, 4, 8, 16, 32, 64, 128, 256)$, $N_{Rx} = 2$, and with $(\alpha_1, \alpha_2) = (0.7, 0.3)$.

CHAPTER FIVE

CONCLUSIONS AND FUTURE WORKS

5.1 Conclusions

In this thesis, two techniques are proposed to enhance the system performance of MIMO-NOMA over mmWave bands, which are cooperative relaying and digital beamforming.

- In the first aspect, wireless communication services have been delivered to users from a BS via a DF-relays by utilizing two links. The first link is from a BS to DF relays, i.e. the backhaul link which uses sub6 GHz mode, while the second link is from the DF relays to users, i.e. access link that exploits mmWave mode with 28GHz or 73 GHz.

- The MIMO-NOMA technique has been used in the backhaul link for a pair of relays that are chosen depending on the proposed pairing algorithm. The signals then have been delivered to the users after applying full detection in the DF relays, which may include SIC depending on the value of PAF allocated to each relay.

- Achievable throughput with error and outage probabilities have been evaluated for this system over different scenarios. Furthermore, MIMO systems with a different number of antennas have been assumed. Comparisons between the two mmWave modes mentioned above have been achieved showing outperforming of 28GHz over 73GHz due to higher attenuation induced by the latter mode.

- The results of this aspect demonstrate the achievable rate that can be obtained over a different number of receiving antennas in all nodes, and over a range of transmitted power from the BS. This would assist significantly to choose the required number of receiving antennas for a particular transmitted power, and verse versa.

- In the second aspect, massive MIMO has been investigated with NOMA and beamforming techniques. A BS that has been equipped with tens of antennas was exploited with ZF and MRT beamforming methods to serve two users in a cluster. Those users and clusters have been chosen by assuming the presence of a pairing algorithm in the BS.

- The BS is also assumed to have full knowledge of the CSI of all users. Depending on these CSI, the BS allocates portions of the total available power between the two users depending on their channel conditions. The proposed system has been analyzed, and the throughput and sum-rate expressions have been expressed.

- The simulation results show a close similarity between the ZF and the MRT in the throughput performance metric, outperforming the MRT when outage probabilities are evaluated. Moreover, the results demonstrate the key role played by increasing the number of antennas in the BS in improving the overall system's performance.

5.2 Future Works

There are several aspects can be considered to extend the proposed systems. These aspects are listed below:

1. Code domain NOMA can be used instead with the power domain type.
2. Other types of cooperative relaying techniques can be considered such as decode amplify-and-forwards (DAF) and compressed-and-forwards (CF).
3. Selected antennas approach for massive MIMO systems can be investigated more to choose the best antennas for transmission.
4. Optimization techniques can be employed for performance reinforcement.
5. Other types of beamforming techniques can be used instead of the utilized methods, such as maximum ratio combining (MRC), hybrid beamforming, and optimum precoding beamforming.

References

[1]   L. Dai, B. Wang, Z. Ding, Z. Wang, S. Chen, and L. Hanzo, "A survey of non-orthogonal multiple access for 5G," *IEEE Commun. Surv. Tutorials*, vol. 20, no. 3, pp. 2294–2323, 2018, doi: 10.1109/COMST.2018.2835558.

[2]   T. Kim, I. Bang, and D. K. Sung, "Design criteria on a mmWave-based small cell with directional antennas," *IEEE Int. Symp. Pers. Indoor Mob. Radio Commun. PIMRC*, vol. 2014-June, pp. 103–107, 2014, doi: 10.1109/PIMRC.2014.7136141.

[3]   C. Seker, M. T. Guneser, and T. Ozturk, "A Review of Millimeter Wave Communication for 5G," *ISMSIT 2018 - 2nd Int. Symp. Multidiscip. Stud. Innov. Technol. Proc.*, pp. 1–5, 2018, doi: 10.1109/ISMSIT.2018.8567053.

[4]   J. Lee, Y. Song, E. Choi, and J. Park, "mmWave cellular mobile communication for Giga Korea 5G project," *2015 21st Asia-Pacific Conf. Commun. APCC 2015*, pp. 179–183, 2016, doi: 10.1109/APCC.2015.7412507.

[5]   M. Ghaddar, L. Talbi, and T. A. Denidni, "Investigation of BS antenna location for future indoor wireless mm-wave communication systems," *IEEE Antennas Propag. Soc. AP-S Int. Symp.*, vol. 2, pp. 110–113, 2003, doi: 10.1109/aps.2003.1219191.

[6]   V. K. Sakarellos, D. Skraparlis, A. D. Panagopoulos, and J. D. Kanellopoulos, "Optimum placement of radio relays in millimeter-wave wireless dual-hop networks," *IEEE Antennas Propag. Mag.*, vol. 51, no. 2, pp. 190–199, 2009, doi: 10.1109/MAP.2009.5162063.

[7]   S. Akoum, O. El Ayach, and R. W. Heath, "Coverage and capacity in mmWave cellular systems," *Conf. Rec. - Asilomar Conf. Signals, Syst. Comput.*, pp. 688–692, 2012, doi: 10.1109/ACSSC.2012.6489099.

[8]   B. Kimy *et al.*, "Non-orthogonal multiple access in a downlink multiuser beamforming system," *Proc. - IEEE Mil. Commun. Conf. MILCOM*, no. 2012, pp. 1278–1283, 2013, doi: 10.1109/MILCOM.2013.218.

[9]   Y. Saito, A. Benjebbour, Y. Kishiyama, and T. Nakamura, "System-level performance evaluation of downlink non-orthogonal multiple access (NOMA)," *IEEE Int. Symp. Pers. Indoor Mob. Radio Commun. PIMRC*, vol. 2, pp. 611–615, 2013, doi: 10.1109/PIMRC.2013.6666209.

[10]   J. Choi, "Non-orthogonal multiple access in downlink coordinated two-point systems," *IEEE Commun. Lett.*, vol. 18, no. 2, pp. 313–316, 2014, doi: 10.1109/LCOMM.2013.123113.132450.

[11]   K. Higuchi, A. Benjebbour, and S. Member, "Non-orthogonal Multiple Access (NOMA) with Successive," *IEICE Trans. Commun.*, vol. Vol. E98-B, no. 3, pp. 403–414, 2015.

[12]   Z. Ding, M. Peng, and H. V. Poor, "Cooperative Non-Orthogonal Multiple Access in 5G Systems," *IEEE Commun. Lett.*, vol. 19, no. 8, pp. 1462–1465, 2015, doi: 10.1109/LCOMM.2015.2441064.

[13]   L. Dai, B. Wang, Y. Yuan, S. Han, C. L. I, and Z. Wang, "Non-orthogonal multiple access for 5G: Solutions, challenges, opportunities, and future research trends,"

IEEE Commun. Mag., vol. 53, no. 9, pp. 74–81, 2015, doi: 10.1109/MCOM.2015.7263349.

[14] S. Sun et al., "Propagation Path Loss Models for 5G Urban Micro- and Macro-Cellular Scenarios," 2016 IEEE 83rd Vehicular Technology Conference (VTC Spring), Nanjing, China, 2016, pp. 1-6, doi: 10.1109/VTCSpring.2016.7504435.

[15] S. Liu and C. Zhang, "Non-orthogonal multiple access in a downlink multiuser beamforming system with limited CSI feedback," *Eurasip J. Wirel. Commun. Netw.*, vol. 2016, no. 1, 2016, doi: 10.1186/s13638-016-0735-9.

[16] H. Zhang, D. K. Zhang, W. X. Meng, and C. Li, "User pairing algorithm with SIC in non-orthogonal multiple access system," *2016 IEEE Int. Conf. Commun. ICC 2016*, 2016, doi: 10.1109/ICC.2016.7511620.

[17] J. Men, J. Ge, and C. Zhang, "Performance Analysis for Downlink Relaying Aided Non-Orthogonal Multiple Access Networks with Imperfect CSI over Nakagami-Fading," *IEEE Access*, vol. 5, pp. 998–1004, 2017, doi: 10.1109/ACCESS.2016.2631482.

[18] K. M. Rabie, B. Adebisi, E. H. G. Yousif, H. Gacanin, and A. M. Tonello, "A Comparison between Orthogonal and Non-Orthogonal Multiple Access in Cooperative Relaying Power Line Communication Systems," *IEEE Access*, vol. 5, pp. 10118–10129, 2017, doi: 10.1109/ACCESS.2017.2710280.

[19] Z. Luo, C. Zhan, L. Zhang, and R. Zhang, "Robust Hybrid Beamforming in Millimeter Wave Relay Networks with Imperfect CSI," *IEEE Access*, vol. 6, pp. 73093–73101, 2018, doi: 10.1109/ACCESS.2018.2881714.

[20] M. A. Almasi and H. Mehrpouyan, "Non-Orthogonal Multiple Access Based on Hybrid Beamforming for mmWave Systems," *IEEE Veh. Technol. Conf.*, vol. 2018-Augus, no. 1, pp. 1–7, 2018, doi: 10.1109/VTCFall.2018.8690549.

[21] K. A. I. Yang, X. Yan, K. Qin, and Q. Wang, "Mimo-Noma in Millimeter-Wave Communication System," *2018 15th Int. Comput. Conf. Wavelet Act. Media Technol. Inf. Process.*, no. 2, pp. 166–169, 2018.

[22] K. Belbase, C. Tellambura, and H. Jiang, "Coverage Analysis of Cooperative NOMA in Millimeter Wave Networks," *IEEE Commun. Lett.*, vol. 23, no. 12, pp. 2154–2158, 2019, doi: 10.1109/LCOMM.2019.2942919.

[23] X. Yu, F. Xu, K. Yu, and X. Dang, "Power Allocation for Energy Efficiency Optimization in Multi-User mmWave-NOMA System with Hybrid Precoding," *IEEE Access*, vol. 7, pp. 109083–109093, 2019, doi: 10.1109/ACCESS.2019.2933328.

[24] L. Zhu, J. Zhang, Z. Xiao, and X. Cao, "User Fairness Non-orthogonal Multiple Access (NOMA) in Millimeter-Wave Communications," *2018 IEEE/CIC Int. Conf. Commun. China, ICCC Work. 2018*, pp. 80–84, 2019, doi: 10.1109/ICCChinaW.2018.8674488.

[25] A. N. Uwaechia and N. M. Mahyuddin, "A comprehensive survey on millimeter wave communications for fifth-generation wireless networks: Feasibility and challenges," *IEEE Access*, vol. 8, pp. 62367–62414, 2020, doi: 10.1109/ACCESS.2020.2984204.

[26] A. A. Amin and S. Y. Shin, "Channel Capacity Analysis of Non-Orthogonal

Multiple Access With OAM-MIMO System," in IEEE Wireless Communications Letters, vol. 9, no. 9, pp. 1481-1485, Sept. 2020, doi: 10.1109/LWC.2020.2994355.

[27] Y. Wang, Z. Tian, and X. Cheng, "Enabling Technologies for Spectrum and Energy Efficient NOMA-mmWave-MaMIMO Systems," *IEEE Wirel. Commun.*, vol. 27, no. 5, pp. 53–59, 2020, doi: 10.1109/MWC.001.2000055.

[28] J. Ghosh, V. Sharma, H. Haci, S. Singh, and I. H. Ra, "Performance Investigation of NOMA Versus OMA Techniques for mmWave Massive MIMO Communications," *IEEE Access*, vol. 9, pp. 125300–125308, 2021, doi: 10.1109/ACCESS.2021.3102301.

[29] M. Han, J. Du, Y. Zhang, X. Li, K. M. Rabie, and G. Nauryzbayev, "Efficient Hybrid Beamforming Design in mmWave Massive MU-MIMO DF Relay Systems with the Mixed-Structure," *IEEE Access*, vol. 9, pp. 66141–66153, 2021, doi: 10.1109/ACCESS.2021.3073847.

[30] J. Hong, P. Yoon, S. Ahn, Y. Cho, J. Na, and J. Kwak, "Three Steps Toward Low-Complexity: Practical Interference Management in NOMA-Based mmWave Networks," *IEEE Access*, vol. 10, no. December, pp. 128366–128379, 2022, doi: 10.1109/ACCESS.2022.3227444.

[31] A. S. Rajasekaran and H. Yanikomeroglu, "Neural Network Aided User Clustering in mmWave-NOMA Systems with User Decoding Capability Constraints," *IEEE Access*, vol. 11, no. April, pp. 45672–45687, 2023, doi: 10.1109/ACCESS.2023.3274556.

[32] W. M. Audu and O. O. Oyerinde, "Modified User Grouping and Hybrid Precoding for Information Decoding and Energy Harvesting in Hardware Impaired Point-To-Point MM-Wave massive MIMO NOMA," *IEEE Access*, vol. 11, on. January, pp. 33741–33756, 2023, doi: 10.1109/ACCESS.2023.3263548.

[33] N. T. Nguyen, H. N. Nguyen, N. L. Nguyen, A. T. Le, T. N. Nguyen, and M. Voznak, "Performance Analysis of NOMA-Based Hybrid Satellite-Terrestrial Relay System Using mmWave Technology," *IEEE Access*, vol. 11, on. January, pp. 10696–10707, 2023, doi: 10.1109/ACCESS.2023.3238335.

[34] T. M. Cover and J. A. Thomas, *Elements of Information Theory*. 2005. doi: 10.1002/047174882X.

[35] W. Liang, Z. Ding, Y. Li and L. Song, "User Pairing for Downlink Non-Orthogonal Multiple Access Networks Using Matching Algorithm," in IEEE Transactions on Communications, vol. 65, no. 12, pp. 5319-5332, Dec. 2017, doi: 10.1109/TCOMM.2017.2744640.

[36] Z. Ding, Z. Yang, P. Fan, and H. V. Poor, "On the performance of non-orthogonal multiple access in 5G systems with randomly deployed users," *IEEE Signal Process. Lett.*, vol. 21, no. 12, pp. 1501–1505, 2014, doi: 10.1109/LSP.2014.2343971.

[37] J. Cheon and H. S. Cho, "Power allocation scheme for non-orthogonal multiple access in underwater acoustic communications," *Sensors (Switzerland)*, vol. 17, no. 11, 2017, doi: 10.3390/s17112465.

[38] X. Zhang and M. Haenggi, "The Performance of Successive Interference Cancellation in Random Wireless Networks," in IEEE Transactions on Information Theory, vol. 60, no. 10, pp. 6368-6388, Oct. 2014, doi: 10.1109/TIT.2014.2341248.

[39] M. AbdelMoniem, S. M. Gasser, M. S. El-Mahallawy, M. W. Fakhr, and A. Soliman, "Enhanced NOMA system using adaptive coding and modulation based on LSTM neural network channel estimation," *Appl. Sci.*, vol. 9, no. 15, pp. 1–19, 2019, doi: 10.3390/app9153022.

[40] S. M. R. Islam, M. Zeng, O. A. Dobre, and K. Kwak, "Nonorthogonal Multiple Access (NOMA): How It Meets 5G and Beyond," *Wiley 5G Ref*, pp. 1–28, 2019, doi: 10.1002/9781119471509.w5gref032.

[41] Y. Fu, Y. Liu, H. Wang, Z. Shi, and Y. Liu, "Mode Selection between Index Coding and Superposition Coding in Cache-Based NOMA Networks," *IEEE Commun. Lett.*, vol. 23, no. 3, pp. 478–481, 2019, doi: 10.1109/LCOMM.2019.2892468.

[42] R. E. Blahut, *Reference Data For Engineers*. Ninth Edition. 2001.

[43] C. Hathway, "Spectral Efficiency," *New Electron.*, vol. 53, no. 3, pp. 27–28, 2020, doi: 10.12968/s0047-9624(22)61115-5.

[44] D. Tse and V. Pramod, *Fundamentals of wireless communication*, vol. 9780521845. 2005. doi: 10.1017/CBO9780511807213.

[45] S. Li, M. Derakhshani, C. S. Chen, and S. Lambotharan, "Outage probability analysis for two-antennas MISO-NOMA downlink with statistical CSI," *2019 IEEE Glob. Commun. Conf. GLOBECOM 2019 - Proc.*, 2019, doi: 10.1109/GLOBECOM38437.2019.9014301.

[46] T. Faculty and M. W. April, "Non-Orthogonal Multiple Access (NOMA) for Cellular Wireless Communications Md Shipon Ali The University of Manitoba in partial fulfillment of the requirements for the degree of Department of Electrical and Computer Engineering," *Thesis*, on. April, 2017.

[47] B. Patnaik, A. Agarwal, S. Mali, G. Misra, and K. Agarwal, "A Review on Non-Orthogonal Multiple Access Technique for Emerging 5G Networks and beyond," *Proc. - Int. Conf. Smart Electron. Commun. ICOSEC 2020*, no. Icosec, pp. 698–703, 2020, doi: 10.1109/ICOSEC49089.2020.9215412.

[48] T. S. Rappaport *et al.*, "Wireless communications and applications above 100 GHz: Opportunities and challenges for 6g and beyond," *IEEE Access*, vol. 7, pp. 78729–78757, 2019, doi: 10.1109/ACCESS.2019.2921522.

[49] I. A. Hemadeh, K. Satyanarayana, M. El-Hajjar, and L. Hanzo, "Millimeter-Wave Communications: Physical Channel Models, Design Considerations, Antenna Constructions, and Link-Budget," *IEEE Commun. Surv. Tutorials*, vol. 20, no. 2, pp. 870–913, 2018, doi: 10.1109/COMST.2017.2783541.

[50] J. Kim, "Millimeter-wave (mmWave) radio propagation characteristics," *Oppor. 5G Networks A Res. Dev. Perspect.*, pp. 461–479, 2016.

[51] F. Gharari, T. M. C. Chu and H. -J. Zepernick, "Performance analysis of a piecewise-and-forward relay network on Rayleigh fading channels," 2015 9th International Conference on Signal Processing and Communication Systems (ICSPCS), Cairns, QLD, Australia, 2015, pp. 1-7, doi: 10.1109/ICSPCS.2015.7391753.

[52] S. Plevel, A. Networks, S. Tomazic, T. Javornik, and G. Kandus, "MIMO : Wireless Communications," on. January 2014, 2008, doi: 10.1081/E-EWMC-120043484.

[53] A. Sha, A. Hafeee, and S. Malarvizh, "VLSI Architecture Of MIMO Antenna

System Based On Square Root Algorithm," vol. 2, no. August, pp. 1900–1903, 2012.

[54] D. Borges, P. Montezuma, R. Dinis, and M. Beko, "Massive mimo techniques for 5g and beyond—opportunities and challenges," *Electronics*, vol. 10, no. 14, pp. 1–29, 2021, doi: 10.3390/electronics10141667.

[55] E. Simon, J. Farah, P. Laly, and G. Delbarre, "A Gradual Resource Allocation Technique for Massive MIMO-NOMA," *IEEE Antennas Wirel. Propag. Lett.*, vol. 21, no. 3, pp. 476–480, 2022, doi: 10.1109/LAWP.2021.3135981.

[56] X. Chen, F. K. Gong, G. Li, H. Zhang, and P. Song, "User Pairing and Pair Scheduling in Massive MIMO-NOMA Systems," *IEEE Commun. Lett.*, vol. 22, no. 4, pp. 788–791, 2018, doi: 10.1109/LCOMM.2017.2776206.

[57] S. P. Jui, "ALGORITHMS FOR ZERO-FORCING BEAMFORMING IN MULTIPLE INPUT MULTIPLE OUTPUT 5G SYSTEMS Faculty of Information Technology," on. October, 2020.

[58] E. Björnson, M. Bengtsson and B. Ottersten, "Optimal Multiuser Transmit Beamforming: A Difficult Problem with a Simple Solution Structure [Lecture Notes]," in IEEE Signal Processing Magazine, vol. 31, no. 4, pp. 142-148, July 2014, doi: 10.1109/MSP.2014.2312183.

[59] J. Li, D. Wang, P. Zhu, and X. You, "Benefits of beamforming training scheme in distributed large-scale MIMO systems," *IEEE Access*, vol. 6, on. January, pp. 7432–7444, 2018, doi: 10.1109/ACCESS.2018.2793845.

[60] E. Ali, M. Ismail, R. Nordin, and N. F. Abdulah, "Beamforming techniques for massive MIMO systems in 5G: overview, classification, and trends for future research," *Front. Inf. Technol. Electron. Eng.*, vol. 18, no. 6, pp. 753–772, 2017, doi: 10.1631/FITEE.1601817.

[61] B. Yang, Z. Yu, J. Lan, R. Zhang, J. Zhou, and W. Hong, "Digital Beamforming-Based Massive MIMO Transceiver for 5G Millimeter-Wave Communications," *IEEE Trans. Microw. Theory Tech.*, vol. 66, no. 7, pp. 3403–3418, 2018, doi: 10.1109/TMTT.2018.2829702.

[62] D. da S. Brilhante *et al.*, "A Literature Survey on AI-Aided Beamforming and Beam Management for 5G and 6G Systems," *Sensors*, vol. 23, no. 9, pp. 1–50, 2023, doi: 10.3390/s23094359.

[63] P. White and G. Reil, "Millimeter-Wave Beamforming: Antenna Array Design Choices & Characterization White Paper," *Measurement*.

[64] A. Bindle, T. Gulati, and N. Kumar, "A detailed introduction of different beamforming techniques used in 5G," *Int. J. Commun. Syst.*, vol. 34, no. 5, pp. 1–10, 2021, doi: 10.1002/dac.4718.

[65] B. D. Rao and M. Yan, "Performance of maximal ratio transmission with two receive antennas," *IEEE Trans. Commun.*, vol. 51, no. 6, pp. 894–895, 2003, doi: 10.1109/TCOMM.2003.813181.

[66] Y. Dursun, F. Fang, and Z. Ding, "Hybrid NOMA based MIMO offloading for mobile edge computing in 6G networks," *China Commun.*, vol. 19, no. 10, pp. 12–20, 2022, doi: 10.23919/JCC.2022.00.024.

[67] Y. Jia, P. Xu, and X. Guo, "MIMO system capacity based on different numbers of

antennas," *Results in Engineering*, vol. 15, on. June, p. 100577, 2022, doi: 10.1016/j.rineng.2022.100577.

[68] Y. Dursun, K. Wang, and Z. Ding, "Secrecy sum rate maximization for a MIMO-NOMA uplink transmission in 6G networks," *Phys. Commun.*, vol. 53, p. 101675, 2022, doi: 10.1016/j.phycom.2022.101675.

[69] T. S. Rappaport, K. Blankenship, and H. Xu, "Propagation and radio system design issues in mobile radio systems for the GloMo project," *Mob. portable radio Res. …*, pp. 1–29, 1997, [Online]. Available: http://citeseerx.ist.psu.edu/viewdoc/download?doi=10.1.1.95.2984&rep=rep1&type=pdf

[70] T. S. Rappaport, G. R. MacCartney, M. K. Samimi, and S. Sun, "Wideband millimeter-wave propagation measurements and channel models for future wireless communication system design," *IEEE Trans. Commun.*, vol. 63, no. 9, pp. 3029–3056, 2015, doi: 10.1109/TCOMM.2015.2434384.

[71] J. He *et al.*, "A tutorial on lossy forwarding cooperative relaying," *IEEE Commun. Surv. Tutorials*, vol. 21, no. 1, pp. 66–87, 2019, doi: 10.1109/COMST.2018.2866711.

[72] E. N. Tominaga, O. L. A. Lopez, H. Alves, R. D. Souza, and J. L. Rebelatto, "Performance Analysis of MIMO-NOMA Iterative Receivers for Massive Connectivity," *IEEE Access*, vol. 10, pp. 46808–46822, 2022, doi: 10.1109/ACCESS.2022.3170715.

[73] R. Verdecia-Peña and J. I. Alonso, "A two-hop mmwave mimo nr-relay nodes to enhance the average system throughput and ber in outdoor-to-indoor environments," *Sensors (Switzerland)*, vol. 21, no. 4, pp. 1–19, 2021, doi: 10.3390/s21041372.

[74] M. A. B. Mohammad, A. A. Osman, and N. A. A. Elhag, "Performance comparison of MRT and ZF for single cell downlink massive MIMO system," *Proc. - 2015 Int. Conf. Comput. Control. Networking, Electron. Embed. Syst. Eng. ICCNEEE 2015*, pp. 52–56, 2016, doi: 10.1109/ICCNEEE.2015.7381427.

Published Articles

[1] **Ahmed A. Saleh, and Mohamad A. Ahmed,** ''*Performance Enhancement of Cooperative MIMO-NOMA Systems over Sub-6GHz and mmWave Bands*'', published in the Journal of Telecommunications and Information Technology (JTIT).

[2] **Ahmed A. Saleh, and Mohamad A. Ahmed,** ''*Multiuser Beamforming System with Massive MIMO-NOMA over mmWave channel*'', accepted for publication in the 2023 1st International Conference on Advanced Engineering and Technologies (ICONNIC), East Java, Indonesia.

الخلاصـة

في هذه الرسالة، تم فحص وتوصيف الوصول المتعدد غير المتعامد (NOMA) مع مدخلات متعددة ومخرجات متعددة (MIMO) عبر قنوات موجة ملليمتر (mmWave). تم دمج هذه التقنيات لخدمة عدد كبير من المستخدمين في الجيل القادم من الاتصالات اللاسلكية. شهدت تقنية تعدد الإرسال NOMA الكثير من الاهتمام نظرًا لقدرتها على تعزيز كفاءة الطيف بشكل كبير. علاوة على ذلك، تعد تقنية MIMO الضخمة آلية الإرسال عبر عشرات ومئات عدد من الهوائيات، مما يحسن أيضًا إنتاجية النظام ويقلل من الطاقة المرسلة المطلوبة. علاوة على ذلك، فإن استخدام mmWave كنطاق واعد غير مزدحم من شأنه أن يعزز أداء النظام ويزيد من عرض النطاق الترددي للإرسال ويقلل من زمن الوصول.

تم اقتراح وتحقيق جانبين في هذه الرسالة، الأول هو استخدام المرحلات التعاونية، في وضع فك التشفير والتقدم (DF)، لمعالجة مشكلة خسارة المسار المتأصلة في نطاقات mmWave، بينما الفكرة الثانية هي لاستخدام تشكيل الحزمة مع MIMO الهائل لتعزيز إشارة المستخدم المطلوب وتقليل التداخل الناتج عن مستخدمين اخرين.

في الجانب الأول، يتم النظر في وصلتين لهما نطاقات تردد مختلفة لخدمة المستعملين بواسطة برج رئيسي (BS) عبر مرحلات تعاونية لتحديد الاتجاه. اقترحت وصلات الربط والوصول مع نطاقي الموجات الفرعية 6 جيجاهرتز وموجة المليمتر (mmWave)، على التوالي. يتم استخدام NOMA في وصلة التوصيل لنقل إشارة متراكبة في مجال الطاقة في نفس الوقت باستخدام نفس النطاق. يتم إنشاء الإشارات المتراكبة، التي تحتوي على إشارتين تختلفان في عوامل توزيع القدرة (PAF)، لمرحلي تحديد الاتجاه المحدد في المحطة القاعدة. يتم اختيار المرحلين من بين عدة مرحلات ليتم استخدامها بواسطة BS عبر استخدام خوارزمية الاقتران اعتمادًا على ظروف المستخدمين المختلفة. يكتشف مرحل DF الأبعد إشارة NOMA الواردة مباشرة، بينما يطبق المستخدم الأقرب عملية إلغاء التداخل المتتالي (SIC) قبل استخراج إشارته. يقوم كل مرحل DF بإعادة توجيه الإشارات المكتشفة نحو المستخدمين المقصودين عبر قنوات mmWave. علاوة على ذلك، يتم استخدام ثلاثة مقاييس للأداء لتقييم أداء النظام، وهي احتمالية الانقطاع، والإنتاجية التي يمكن تحقيقها، ومعدل الخطأ في البت.

علاوة على ذلك ، تم الحصول على مقارنات بين نطاقي mmWave في ارتباط الوصول، وهما 28 جيجاهرتز و 73 جيجاهرتز، لإثبات تفوق 28 جيجاهرتز في مقاييس الأداء الثلاثة.

في الجانب الثاني، يُعتبر MIMO الهائل مع NOMA لخدمة العديد من المستخدمين لاسلكيًا عبر قنوات mmWave، حيث يُقترح BS مع عشرات الهوائيات لتوفير الخدمات للمستخدمين في منطقة التغطية من خلال تطبيق التأثير الصفري (ZF) والنسبة القصوى تقنيات تشكيل حزم الإرسال (MRT). تقسم BS المنطقة أولاً إلى مجموعات تحتوي على مستخدمين فقط من خلال تطبيق خوارزمية الاقتران، ثم يتم تطبيق NOMA على المستخدمين الاثنين من خلال توفير عوامل تخصيص طاقة مختلفة لإرضاء عدالة المستخدم، واعتمادًا على ظروف المستخدمين. يتم تحليل وتقييم الإنتاجية التي يمكن تحقيقها لكل مستخدم في المجموعة جنبًا إلى جنب مع معدل المجموع الذي توفره المحطة القاعدة لآليتي تشكيل الحزمة. تم الحصول على النتائج لأعداد مختلفة من هوائيات المحطة القاعدة على توليفات مختلفة من معاملات توزيع القدرة. تكشف نتائج المحاكاة عن التحسن الناتج عن زيادة الهوائيات في المحطة القاعدة. بالإضافة إلى ذلك، تقدم طريقتنا تشكيل الحزمة انتاجية متشابهةً عند استخدام نفس المتغيرات تحت نفس الظروف، مع تفوق طفيف لل MRT بمقياس احتمالية الانقطاع.

إقرار لجنة المناقشة

نشهد بأننا أعضاء لجنة التقويم والمناقشة قد اطلعنا على هذه الرسالة الموسومة" **إستقصاء ومحاكاة الاداء القائم على الوصول المتعدد غير المتعامد (NOMA) عبر قنوات الموجات الملميترية**" وناقشنا الطالب (**احمد عطاالله صالح**) في محتوياتها وفيما له علاقة بها بتاريخ / /2023 وقد وجدناه جديراً بنيل شهادة الماجستير–علوم في اختصاص هندسة الاتصالات.

التوقيع:

رئيس اللجنة: أ.م.د ضياء محمد علي

التاريخ: / /2023

عضو اللجنة: أ.م.د سعد احمد ايوب

التوقيع:

عضو اللجنة: أ.م.د صفوان حفيظ يونس

التاريخ: / /2023

عضو اللجنة(المشرف): أ.م.د.محمد عبدالرحمن

التاريخ: / /2023

قرار مجلس الكلية

اجتمع مجلس كلية هندسة الالكترونيات بجلسته المنعقدة بتاريخ : / /2023

وقرر المجلس منح الطالب شهادة الماجستير علوم في اختصاص هندسة الاتصالات.

التوقيع:

مقرر المجلس:أ.م.د. بلال علاء الدين جبر

التاريخ: / /2023

رئيس مجلس الكلية: أ.د. خالد خليل محمد

التاريخ: / /2023

إقرار المشرف

اشهد بان الرسالة الموسومة بـ " **استقصاء ومحاكاة الاداء القائم على الوصول المتعدد غير المتعامد**
(NOMA) عبر قنوات الموجات الملميترية " تم اعدادها من قبل الطالب **(احمد عطاالله صالح)**
تحت اشرافي وهي جزء من متطلبات نيل شهادة الماجستير في هندسة الاتصالات.

التوقيع:

المشرف: أ.م.د. محمد عبدالرحمن احمد الحبار

التاريخ: /   / 2023

إقرار المقيم اللغوي

اشهد باني قمت بمراجعة الرسالة الموسومة بـ " **استقصاء ومحاكاة الاداء القائم على**
الوصول المتعدد غير المتعامد (NOMA) عبر قنوات الموجات الملميترية " من الناحية
اللغوية وتصحيح ما ورد فيها من أخطاء لغوية وتعبيرية وبذلك أصبحت الرسالة مؤهلة للمناقشة
بقدر تعلق الامر بسلامة الأسلوب وصحة التعبير.

التوقيع :

المقوم اللغوي: م.محمد نظير محمود

التاريخ: /   / 2023

إقرار رئيس لجنة الدراسات العليا

بناء على التوصيات المقدمة من قبل المشرف والمقوم اللغوي أرشح هذه الرسالة للمناقشة.

التوقيع:

الاسم: أ.م.د. محمود احمد محمود

التاريخ: /   / 2023

إقرار رئيس القسم

بناء على التوصيات المقدمة من قبل المشرف والمقوم اللغوي ورئيس لجنة الدراسات العليا أرشح هذه
الرسالة للمناقشة.

التوقيع:

الاسم: أ.م.د. محمود احمد محمود

التاريخ: /   / 2023

وزارة التعليم العالي والبحث العلمي

جامعة نينوى

كلية هندسة الالكترونيات

قسم هندسة الاتصالات

استقصاء ومحاكاة الاداء القائم على الوصول المتعدد غير المتعامد (NOMA) عبر قنوات الموجات الملميترية

رسالة تقدم بها

احمد عطاالله صالح

إلى

مجلس كلية هندسة الالكترونيات

جامعة نينوى

كجزء من متطلبات نيل شهادة الماجستير

في

هندسة الاتصالات

بإشراف

أ.م.د. محمد عبدالرحمن احمد الحبار

1445 هـ   2023م

استقصاء ومحاكاة الاداء القائم على الوصول المتعدد غير المتعامد (NOMA) عبر قنوات الموجات الملميترية

احمد عطاالله صالح

رسالة ماجستير علوم في هندسة الاتصالات

بإشراف

أ.م.د. محمد عبدالرحمن احمد الحبار

1445 هـ 2023م